Optimal Rate Allocation for Production and Injection Wells in an Oil and Gas Field for Enhanced Profitability

Optimal Rate Allocation for Production and Injection Wells in an Oil and Gas Field for Enhanced Profitability

Emmanuel I. Epelle and Dimitrios I. Gerogiorgis*

Institute for Materials and Processes (IMP), School of Engineering, University of Edinburgh, The King's Buildings, Edinburgh, EH9 3FB, United Kingdom

**Corresponding author: D.Gerogiorgis@ed.ac.uk (+44 131 6517072)*

ABSTRACT

An oil and gas field requires careful operational planning and management via production optimisation for increased recovery and long-term project profitability. This paper addresses the challenge of production optimisation in a field undergoing secondary recovery by water flooding. The field operates with limited processing capacity at the surface separators, pipeline pressure constraints and water injection constraints; an economic indicator (Net Present Value – NPV) is used as the objective function. The formulated optimisation framework adequately integrates slow-paced subsurface dynamics using reservoir simulation and the fast-paced surface dynamics using sophisticated multiphase flow simulation in the upstream facilities. Optimisation of this holistic long–term model is made possible by developing accurate second order polynomial proxy models at each time step. The resulting formulation is solved as a Nonlinear Program (NLP) using commercially available solvers. A comparative analysis is performed using MATLAB's fmincon solver and the IPOPT solver for their robustness, speed and convergence stability in solving the proposed problem. By implementing 2 synthetic case studies, our mathematical programming approach determines the optimal production and injection rates of all wells and further demonstrates considerable improvement to the NPV obtained by simultaneously applying the tools of streamline, reservoir and surface facility simulation for well rate allocation.

Introduction

It is estimated that oil companies produce up to three barrels of water for each barrel of oil from depleting reservoirs, and this costs approximately $40 billion annually to handle (Bailey et al., 2000). Field engineers in the oil and gas industry are constantly faced with the challenge of maintaining profitability amidst several operational constraints, such as the optimal water injection strategy for mature fields undergoing secondary production. The effects of these constraints span through all time horizons. With inevitably high environmental and financial stakes associated with the exploration and production of mature oil and gas fields, there is a strong incentive to enhance hydrocarbon recovery and production via systematic and mathematical-oriented approaches. [1-2] In further response to this challenge, the application of sophisticated simulation methodologies to integratedly capture the reservoir behaviour, multiphase flows (in wellbores and flowlines) and gas-oil-water separation in the processing facilities is constantly on the increase. [3–5] Liquid loading in gas wells and artificial lift design considerations, reservoir pressure maintenance via water injection, gas/water coning during production from vertical and horizontal wells, pressure drop and liquid holdup of multiphase mixtures in highly deviated flowlines are some of the specific complexities associated with this system.

Simulation of these prevalent subsurface and surface phenomena does not always guarantee an accurate prediction of the on-set of these problems, let alone, a problem-free operation in a field. In order to tackle the insufficiencies and thus reduce the uncertainties of the current state-of-the-art models, it is necessary to also combine robust optimisation methods with these flow simulations. [6–7] This combination of simulation and optimisation algorithms increases complexity due to function evaluations, lack of gradient information, model nonlinearity, non-convexity and the presence of discrete and binary routing variables.

Beyond several notable contributions, the work presented here is premised on industrial findings that, controlling injected water rates and hence volumes of produced water is one of the fastest and least expensive ways to reduce field operating costs and increase hydrocarbon recovery simultaneously. [8] This ultimately depends on the production and injection rates of the wells, rock and fluid properties, the method of water handling amongst many other factors. Hence, exploiting a process systems

engineering description of the problem aids operational decisions by providing an optimal production and water injection strategy for the considered case studies. By applying sound mathematical-oriented optimisation methods, the dependence on heuristic-based diagnostic methods for production and water injection control can be reduced and thus, used as a complementary tool.

Literature Review

The highly diverse range of research efforts targeted towards field production optimisation from a reservoir to surface facility perspective can be generally grouped into short-term and long-term optimisation scenarios. A further classification could comprise field studies undergoing primary production and others with some secondary enhancement. Furthermore, some studies consider production optimisation by only analysing hydrocarbon flow from reservoir to wellbore without constraints on processing facilities. It is also possible to classify existing studies based on the type of problem tackled, which include: well placement, rate allocation/production planning and scheduling, pipeline and surface facility routing, drilling and drill rig scheduling, infrastructure installation under geological and economic uncertainty. As a result of the highly interconnected nature of these classifications, relevant studies that fall within the listed categories, are discussed.

Barragan-Hernandez et al. formulated a model for the simulation and optimisation of oil and gas production systems.[9] An one-day operating period has been considered in their publication: therein, important phenomena (such as reverse flow and critical flow in valves) were also modelled, using a set of differential-algebraic equations and thermodynamic state calculations in a detailed case study.

Nikolaou and coworkers have extensively addressed the dire need to bridge the gap between petroleum reservoir modelling and real-time production optimisation, exploring successfully several fruitful ideas, most notably the moving-horizon concept and the parametric and automated adaptive modelling approaches. [10–14]

Gunnerud et al. proposed a disaggregated framework for optimising an entire production network over a short-term horizon at steady state conditions. [1] This computational framework which is also adopted in the present paper analyses the entire system as a combination of wells, pipelines and

separators. Several rigorous model approximation methods (e.g. linear interpolation, spline interpolation, algebraic proxy modelling and Special Ordered Sets/SOS, SOS2 approximations) have been implemented in similar papers. [1, 6–7, 15–16] Silva and Camponogara (2014) addressed the optimisation of gas lifted wells under facility, routing and pressure constraints.[17] Single-dimensional and multidimensional piecewise approximations for pipelines and wellbores have been used therein to compute pressure drops. As demonstrated by Codas et al., integrated production optimisation problems can be solved rapidly for real time application. [18] Therein, the optimisation framework considers a production system with complex routing, capacity and pressure constraints, and with wells exhibiting coning behaviour. Despite these proposed developments, little attention is given to fields exploited via secondary oil and gas production methods.

Tavallali et al. have tackled well placement, production planning, and facility allocation optimisation problems [2, 19–21] using an open-box approach which involves a problem-specific modification of the outer approximation algorithm proposed by Grossmann and co-workers. [22–24] Furthermore, long-term infrastructure planning and production scheduling challenges have also been addressed in several publications by Grossmann and coworkers via complex MILP and MINLP formulations. [25–30] Although the productivity index of wells in a field is bound to change with time in practical field operations, the paper by Iyer and Grossmann assumes a constant productivity index (PI) for all the wells and the entire long-term horizon. [25] A time-dependent PI approach is thus adopted in the present paper, to offer a more comprehensive approach when the foregoing assumption becomes restrictive. Joint optimisation of well placement and rate control has been studied recently by Bellout et al.: they demonstrated that embedding well control optimisation within optimal well placement configurations yields up to 20% improvement in NPV compared to sequential approaches. [31] Geological uncertainty has been explored by Li et al., who used a Simultaneous Perturbation Stochastic Algorithm (SPSA). [32]

Several geological realisations and numerical experiments have also been employed in order to further demonstrate improved performance obtainable by solving well placement and rate control optimisation problems simultaneously. The impact of economic uncertainty with reference to the market price of oil and gas, field size and eventual deliverability has been addressed by Gupta and

Grossmann. [30] A complex economic objective function with business considerations has been adopted therein towards enhancing planning decisions over a field's lifetime. Moreover, an adaptive simulated annealing algorithm was employed by Azamipour et al., for the production optimisation of a field undergoing water injection: therein, optimisation time reduction was attained by sequentially implementing coarse and fine grids without discernible loss in model accuracy. [33] The authors improved their optimisation approach in a subsequent paper, using a hybrid genetic algorithm. [34] As part of their improvements, streamline simulation has also been adopted for the determination of good initial guesses for the water injection rates. Nevertheless, these contributions do not account for oil and gas surface production facilities. Furthermore, multiphase flow complexity in deviated well geometries is generally not considered in the literature: this indicates a clear opportunity to address multiscale complexity in detail, towards exploring and demonstrating stronger benefits. [35–36]

Subsurface technological advances induce new methodological and computational challenges: therefore, reservoir simulators and advanced optimal operation approaches have also been developed specifically so as to address the geological uncertainty ubiquitous in unconventional reservoirs. [37–39]

An alternative but also fruitful approach for real-time optimisation of these (inherently dynamic) oil and gas production systems is to use feedback and Model-Predictive Control (MPC) formulations, particularly when in-situ instrumentation is available to provide high-frequency output variable data (especially in the presence of mixed timescales, as is the case in hydraulic fracturing before the onset of actual hydrocarbon production.) [40–42] Model order reduction strategies based on detailed (albeit computationally intractable) PDE descriptions can be employed to serve such MPC formulations. [43–44]

In this paper, we provide novel insight into the two highlighted limitations of past studies by formulating and solving a long-term, multi-period production optimisation problem via simultaneous consideration of production and injection wells with both vertical and deviated geometries. We utilise the tools of multiphase flow and reservoir simulation for the flowrate and pressure drop evaluation in wellbores and flowlines of the considered production network; extra measures are taken in the adopted simulation methodology to ensure that all flowlines are free from hydrates at the prevalent temperature and pressure conditions. The problem is solved as a nonlinear program (NLP) comprising

of an economic objective function and several constraints to ensure operational feasibility. The adopted optimisation technique yields enhanced profitability via production and water injection optimisation; thus, demonstrating the efficiency of the proposed method as a value addition tool.

Methodology

Modeling a typical production system

Fig. 1, illustrates a typical production system involving the flow of hydrocarbons over a sufficient pressure gradient from the reservoir to the separators operating at a known constant pressure. To model this complex system, pressure and flowrates can be analysed by decomposing the system into two main rigorously modelled sections. First, is the reservoir to wellbore flow section as described mathematically by the well's Productivity Index (PI), Vertical Flow Performance and Inflow Performance Relationship (IPR), respectively (Fig. 2). Eqs. 1, 2 and 3 are the PI calculation methods for an oil well, a gas well and an oil well operating below its bubble point (Vogel's IPR).

Figure 1: Production system architecture.

Just as the Productivity Index (PI) characterises the performance of a production well, the Injectivity Index (II) is a performance indicator of water injection wells (Eq. 4); we assume an incompressible water phase and the injection pressure is below the formation's fracture pressure. Injector efficiency (via streamline simulation) is another performance metric for injection wells considered here.

In Eqs. 1-11, Q_o represents the oil production rate from a well, which could be vertical, Q_{ov} or horizontal, Q_{oh}. P_r is the average reservoir pressure, P_{wf}, the bottomhole flowing pressure, r_e, the radius of drainage, r_{eh}, the effective drainage radius of a horizontal well, and r_w, the wellbore radius. The oil and gas viscosities are denoted as μ_g and μ_o, respectively. The net thickness of the formation is represented as h, k_h is the horizontal permeability, k_v is the vertical permeability and k is the geometric average permeability; s is the total skin, Z is the gas deviation factor at an average temperature, T; B_o and B_g are the oil and gas formation volume factors, respectively. For horizontal wells, L is the horizontal well length, and a is half the distance of the major axis of the drainage ellipse. [45]

Figure 2: Inflow Performance Relationship (IPR) and Vertical Flow Performance (VFP) curves.

$$PI_L = \frac{Q_o}{(P_r - P_{wf})} \tag{1}$$

$$PI_G = \frac{Q_g}{({P_R}^2 - {P_{wf}}^2)} \tag{2}$$

$$Q_o = Q_b + \left(\frac{PI \times P_b}{1.8}\right)\left[1 - 0.2\frac{P_{wf}}{P_b} - 0.8\left(\frac{P_{wf}}{P_b}\right)^2\right] \tag{3}$$

$$Q_w = II_W \times (P_{wf} - P_r) \tag{4}$$

The flowrates of the respective fluids from the reservoir are dependent on the reservoir properties as shown in Eq. (5–8) and are based on Darcy's law. For horizontal wells, a more complex relationship exists between the productive length of a well and its productivity index (Eqs. 7 and 8).

The multiphase flow description of produced fluids in pipelines under varying inclinations and flow regimes employs robust multiphase correlations (Eq. 12). Optimisation of a coupled system of equations representing both sections is a highly challenging task, for which several solution approaches have been proposed. The increasing number of contributions can be attributed to the advances in the development of specialised algorithms, accompanying computational power and most importantly proxy modelling techniques (polynomials, spline kriging, Artificial Neural Networks). A detailed description of our system components modelling and simulation strategy follows.

$$Q_{ov} = \frac{7.08 \times 10^{-3} k_h h(P_r - P_{wf})}{\mu_o B_o \left[ln\left(\frac{r_e}{r_w}\right) - 0.75 + s\right]} \tag{5}$$

$$Q_{gv} = \frac{7.03 \times 10^{-4} k_h h(P_r^2 - P_{wf}^2)}{\mu_g ZT \left[ln\left(\frac{r_e}{r_w}\right) - 0.75 + s\right]} \tag{6}$$

$$Q_{oh} = \frac{7.08 \times 10^{-3} k_h h(P_r - P_{wf})}{\mu_o B_o \left\{ln\left[\frac{a + \sqrt{a^2 - \left(\frac{L}{2}\right)^2}}{\left(\frac{L}{2}\right)}\right] + \frac{\beta h}{L} ln\left(\frac{\beta h}{(\beta + 1) r_w}\right)\right\}} \tag{7}$$

$$Q_{gh} = \frac{7.06 \times 10^{-4} k_h h(P_r^2 - P_{wf}^2)}{\mu_g ZT \left\{ln\left[\frac{a + \sqrt{a^2 - \left(\frac{L}{2}\right)^2}}{\left(\frac{L}{2}\right)}\right] + \frac{\beta h}{L} ln\left(\frac{\beta h}{(\beta + 1) r_w}\right)\right\}} \tag{8}$$

$$a = \frac{L}{2}\left[0.5 + \sqrt{0.25 + \left(\frac{2r_{eh}}{L}\right)^4}\right]^{0.5} \tag{9}$$

$$\beta = \sqrt{\frac{k_h}{k_v}} \tag{10}$$

$$k = \sqrt{(k_h k_v)} \tag{11}$$

$$\left(\frac{dP}{\mathrm{dL}}\right)_{total} = \left(\frac{dP}{\mathrm{dL}}\right)_{friction} + \left(\frac{dP}{\mathrm{dL}}\right)_{gravity} + \left(\frac{dP}{\mathrm{dL}}\right)_{acceleration} \tag{12}$$

Reservoir Simulation

Before applying mathematical optimisation, we adopt reservoir engineering tools (PETREL®,[46] ECLIPSE® 100,[47] and FrontSIM® [48]) for modelling fluid flow in porous media. [46–48] Firstly, we construct and discretise the reservoir (using PETREL® [46]) and run a test forecast simulation (using ECLIPSE® 100 [47]) to determine performance of each well and the increment in oil production due to water flooding – 'x' (Fig. 3a). This increment is obtained at each time step (Δt). In running this test case for the determination of initial guesses, we first adopt a constant injection rate over the entire time horizon (Fig. 3c-i), and then apply injection rates derived from efficiency calculations.

Figure 3: Oil production and water injection profiles in the reservoir; Δt is taken to be 365 days.

In order to perform porous media flow simulations of the water flooding process, the following set of nonlinear material balance equations, in each cell (Figs. 9 and 12) are solved for each phase.

$$\sum_{l\in\psi_n} T_{o_{f,n}}^{n+1}\left[(p_{o_f}^{n+1} - p_{o_n}^{n+1}) - \gamma_{o_{l,n}}^{n}(Z_f - Z_n)\right] + \sum_{f\in\xi_n} q_{osc_{f,n}}^{n+1} + q_{osc_n}^{n+1} = \frac{V_{b_n}}{\alpha_c \Delta t}\left\{\left[\frac{\varphi(1-S_w-S_g)}{B_o}\right]_n^{n+1} - \left[\frac{\varphi(1-S_w-S_g)}{B_o}\right]_n^{n}\right\} \tag{13}$$

$$\sum_{f\in\psi_n} T_{w_{f,n}}^{n+1}\left[(p_{o_f}^{n+1} - p_{o_n}^{n+1}) - \left(P_{cow_f}^{n+1} - P_{cow_n}^{n+1}\right) - \gamma_{w_{f,n}}^{n}(Z_f - Z_n)\right] + \sum_{f\in\xi_n} q_{wsc_{f,n}}^{n+1} + q_{wsc_n}^{n+1} = \frac{V_{b_n}}{\alpha_c \Delta t}\left\{\left[\frac{\varphi(S_w)}{B_w}\right]_n^{n+1} - \left[\frac{\varphi(S_w)}{B_w}\right]_n^{n}\right\} \tag{14}$$

$$\begin{aligned}\sum_{f\in\psi_n} T_{g_{f,n}}^{n+1}&\left[(p_{o_f}^{n+1} - p_{o_n}^{n+1}) + \left(P_{cgo_f}^{n+1} - P_{cgo_n}^{n+1}\right) - \gamma_{g_{f,n}}^{n}(Z_f - Z_n)\right] \\ &+ (T_o R_s)_{f,n}^{n+1}\left[(p_{o_f}^{n+1} - p_{o_n}^{n+1}) - \gamma_{o_{f,n}}^{n}(Z_f - Z_n)\right] + \sum_{l\in\xi_n}\left[q_{fgsc_{f,n}}^{n+1} + R_{s_n}^{n+1} q_{osc_{f,n}}^{n+1}\right] \\ &+ \left[q_{fgsc_{f,n}}^{n+1} + R_{s_n}^{n+1} q_{osc_{f,n}}^{n+1}\right] \\ &= \frac{V_{b_n}}{\alpha_c \Delta t}\left\{\left[\frac{\varphi(S_g)}{B_g}\right]_n^{n} - \left[\frac{\varphi(S_g)}{B_g}\right]_n^{n} + \left[\frac{\varphi R_s(1-S_w-S_g)}{B_o}\right]_n^{n+1} - \left[\frac{\varphi R_s(1-S_w-S_g)}{B_o}\right]_n^{n}\right\}\end{aligned} \tag{15}$$

Reservoir modelling assumptions

- Reservoir rock and fluid (light oil/gas) properties (Table 1) are available (3D dimensions, absolute and relative permeability data, porosity, fluid density, viscosity, compressibility, oil/gas formation volume factors, reservoir initial pressure, residual water and gas saturations).
- The reservoir is considered infinite acting with no near-by boundaries such as faults present.
- Number and locations of producers and injectors are known; all wells are drilled at the same time and commence operation (production and injection) simultaneously.
- Production time horizon is known (T = 6 years).
- Capillary pressure effects are insignificant in the reservoir.
- Economic parameters such as the unit volumetric costs for oil and gas sales and water treatment costs are available.

Table 1: Fluid and reservoir properties.

Figure 4: Statistical distributions of porosity (a), horizontal (b) and vertical permeability (c).

Streamline simulation

Streamlines describe the tangential velocity vectors in a field at any point in time by solving a 1D transport problem along each line. [49] Thus, multiphase flow effects can be captured, portraying variable well production rates and the underlying permeability distribution.

Time-dependent Well Allocation Factors (WAFs) between injection and production wells can be derived from the results of the streamline simulation and used for the calculation of the injection efficiency (IE). [49] Through the use of this performance indicator, it is possible to determine how much additional oil can be produced per unit volume of water injected by an offset injector.

$$IE = \frac{offset\ oil\ production}{water\ injection} \tag{16}$$

$$IE = \frac{\sum_{j=1}^{J}(WAF_{j,i} \times q_{o,j})}{q_{w,i}} \tag{17}$$

$$WAF_{j,i} = \frac{Number\ of\ streamlines\ connecting\ producer, j\ \ and\ injector, i\ (N_{p,i})}{Number\ of\ streamlines\ for\ producer, j\ (N_P)} \quad (18)$$

Although we aim to optimise the production-injection-surface facility network using a classical optimisation algorithm, the number of variables involved implies that their initial guesses significantly affect the quality of the solution obtained. Hence, streamline simulation (using FrontSIM® [48]) is implemented for the generation of more reliable initial guesses, in the interest of rapid convergence of the optimisation algorithm. Well rates computed using the reservoir simulator (ECLIPSE® 100 [47]) serve as good starting points for the optimiser. Improved oil recovery is thus possible by employing mathematical optimisation which relies on high-fidelity, first-principles reservoir simulations.

With the calculated injector efficiency at each timestep, and the total daily available water capacity, a reliable injection rate estimates at each time step can be determined (Fig. 3c-ii). The latter can be used to re-run a forecast of the field's oil production and obtain Productivity Indices (PI) of production wells, the field's Gas Oil Ratio (GOR) and Water Cut (WC) as functions of time.

Incorporating Wellbore Hydraulics

Subsequent to obtaining the above listed parameters at each time step, is the use of a multiphase flow simulator (PIPESIM® [52]) to estimate pressure drops in the wellbores and pipelines, respectively. The PI, II, GOR, WC at each timestep are required inputs to PIPESIM® [52] for pressure drop calculations.

Figure 5: Well schematic showing completion details for pressure drop estimation.

The well trajectory and well completion details (casing size, tubing size and perforation intervals), are also imported from PETREL® [46] and used in the pressure drop calculations in PIPESIM®.[52] A sensitivity analysis is run on the wells and pipelines to obtain high resolution data tables at each time step. Table 2 shows the data construction strategy for the wells.

Table 2: Structure of data obtained for each well and pipeline from PIPESIM® at each timestep

Datasets obtained are imported into MATLAB and multivariate nonlinear regression yields polynomial proxy models (all wells assumed connected to one pipeline without routing constraints).

Proxy modelling and the optimisation framework

Proxy modelling is increasingly becoming applicable to highly complex processes such as a petroleum production system with many variables per system component. However, the requirements of a proxy model are usually high since it is desired that they capture highly nonlinear system behaviour embedded in a relatively low number of representative samples/original simulation runs. [52] The entire optimisation problem can be divided in four elements: (a) subsurface flow dynamics, (b) wellbore flow dynamics, (c) surface flow pressure drops, (d) economic considerations. Besides the economic considerations reflected in the objective function of the problem, numerous reservoir and multiphase flow simulations are required to capture the reservoir, well and surface dynamic behaviour. Running these complex and rigorous simulations within an optimisation routine is expensive computationally. This disadvantage can be overcome by developing robust proxy models (simplified response surface representations) of similar accuracy with the simulators.

To circumvent the unnecessary complexity of coupling the interface of all simulators used in this work, it was necessary to generate high resolution data tables for the proxy modelling phase before calling the optimisation algorithm. Up to 30 different wellhead pressures/surface injection pressures (for the producers and injectors, respectively) and 50 different liquid production rates (within practical and acceptable ranges) were used for the development of the proxy models, thus yielding a total of 3060 simulations for the different phases, at the respective time intervals.

The study by Yeten et al. indicates that quadratic polynomials (especially those with cross-terms) offer comparable performance to other complex response surfaces (kriging, splines and ANN), when a space-filling design methodology is applied. [51] They attributed this performance of quadratic polynomials to the fact that they are not data-sensitive, nor severely affected by instantaneous local changes in erratic data compared to kriging and splines in regard to local high-gradient satisfaction.

In order to improve the accuracy of the parameter estimation procedure for the pipeline proxy models, a sub-optimisation problem is formulated using a genetic algorithm for error minimization between simulator data and proxy model data using the regression results as initial guesses. The error function

is given by Eq. 19, where *MD* represents the mean deviation, *SD*, the simulation data, and *PD*, the proxy model data. The structure of the proxy models used for the wells and pipelines are shown in Eqs. 26-28, respectively: The simulation-based optimisation methodology is shown in Figs. 6-7.

$$MD = \frac{|SD - PD|}{SD} \times 100 \tag{19}$$

Objective Function

$$\max(NPV) = \sum_{t=1}^{N_t} \left[\frac{TOP^t + TGP^t - (TWP^t + TWI^t)}{(1+b)^{\frac{t}{t_{ref}}}} \times \Delta t \right] \tag{20}$$

$$TOP^t = r_{op} \times \sum_{j=1}^{Nprod} q_{op,j,t} \tag{21}$$

$$TGP^t = r_{gp} \times \sum_{j=1}^{Nprod} q_{gp,j,t} \tag{22}$$

$$TWP^t = r_{wp} \times \sum_{j=1}^{Nprod} q_{wp,j,t} \tag{23}$$

$$TWI^t = r_{winj} \times \sum_{i=1}^{Ninj} q_{winj,i,t} \tag{24}$$

3.5.2 Constraints:

$$\sum_{j=1}^{Nprod} q_{gp} \leq C_{g,sep} \tag{25}$$

$$q_{p,j,t} = a_1 + a_2 P_{j,t}^w + a_3 (P_{j,t}^w)^2 \tag{26}$$

$$q_{p,j,t} = b_1 + b_2 P_{i,t}^w + b_3 (P_{i,t}^w)^2 \tag{27}$$

$$\Delta P_{l,t} = c_1 + c_2 q_{lg,t} + c_3 q_{lo,t} + c_4 q_{lw,t} + c_5 (q_{lg,t})^2 + c_6 (q_{lo,t})^2 + c_7 (q_{lw,t})^2 + c_8 q_{lg,t} q_{lw,t} + c_9 q_{lg,t} q_{lo,t} + c_{10} q_{lo,t} q_{lw,t} \tag{28}$$

$$P^s = P^m - P_{l,t} \tag{29}$$

$$P^m < P_j^w \tag{30}$$

$$P_{inj} < P_{frac} \tag{31}$$

$$\sum_{j=1}^{Nprod} q_{p,j,t} = q_{p,l,t} \tag{32}$$

$$\sum_{i=1}^{Ninj} q_{winj} \leq Q_{inj,tot} \tag{33}$$

The present paper adopts a simulation-based optimisation method based on the respective one by Gunnerud, Foss and coworkers, in which the production network is broken down into several black boxes in order to formulate explicit relations, rather than treating the entire network as a single black

box.[1,5] They argue that although proxy models are required for each section of the entire production network, configuring the optimiser to search using smaller simulators yields faster computations compared to searching over the entire production network. The surrogate modelling approach adopted here also offers a clear opportunity for implementation of a gradient-based optimisation solver.

The control variables include choke valve settings at the wellhead which ensure there is no material back flow, gas and water handling capacity constraints and pressure bounds on the pipelines. The algorithm aims to determine the optimum injection profile that maximises the oil production and the field revenue in terms of the NPV. Eqs. 19-24 represent the well flow rates for each phase as a function of the wellhead pressures. This has been obtained by running a nodal analysis in PIPESIM®[52] at different wellhead pressures and subsequently developing a quadratic proxy model by regressing the data. Similarly, the nonlinear relationship between the pipeline pressure drop and the flow rates of the respective phases is obtained by running a sensitivity analysis in PIPESIM® [52] (P/T profile or system analysis) at different pipeline liquid flow rates. Eq. 32 is a mass balance constraint ensuring the well flows of respective phases are routed to the pipeline between the manifold and the separator. It is also necessary to constrain the manifold pressure (Eq. 30), ensuring forward flow of all phases for the wells. The available water for injection in the field is limited to 10,000 STB/day (Eq. 33).

The results of the optimisation problem (NLP) are the optimal production and injection rates that satisfy all constraints and maximise the objective function. With the practical initial guesses obtained by applying reservoir simulation, we propose bounds to the decision variables, assume a uniform distribution between the upper and lower bounds of the respective variables and perturb the initial guesses 1000 times between the bounds, facilitating convergence. We also compare the performance of the 'IPOPT' solver and MATLAB's 'fmincon' subroutine (required iterations, solution times).

Figure 6: Coupling procedure. *P*, reservoir pressure, *Q*, flowrates and *R*, ratios (WC & GOR).

The optimisation procedure was carried out using the OPTI toolbox platform in MATLAB, for interfacing with the Interior Point Optimiser (IPOPT solver). The default MATLAB fmincon solver (with the interior point algorithm) in MATLAB was also implemented for comparison purposes.

Figure 7: Summary of simulation and optimisation methodology

The implementation of the interior point algorithm in MATLAB involves a solution of a sequence of approximate optimisation problems (equality-constrained problems) which are easier to solve than the original inequality-constrained problem. To solve the approximate problem, the algorithm attempts to take a direct step (Newton step) first, which if unsuccessful results in the application of a conjugate gradient step using a trust region. The IPOPT solver on the other hand implements an interior point line-search filter method; the interested reader is referred to the mathematical formulation of the algorithm documented in several publications.[53–56] The solver implements a two-phase algorithm which comprises a main phase and a feasibility restoration phase. In the main phase, the classical infeasibility start method is used to simultaneously search for optimality and feasibility; whereas, the feasibility restoration phase seeks to minimize primal infeasibility. This phase is only called when the main phase fails. The main drawback of the algorithm is the difficulty of detecting infeasibility; it often fails when the feasibility restoration phase is called too close to the optimal solution.[57] Although several modifications to the algorithm (e.g. the one-phase interior point method for nonconvex optimisation) have been proposed,[57–58] the two-phase algorithm has been sufficiently robust for the purpose of this paper, allowing us to solve all case studies to convergence within a reasonable time.

Problem Description

Case Study 1 (CS 1)

The petroleum field considered here is one undergoing secondary production with already located 3 producer wells and 1 injector well. The reservoir is primarily sandstone with established properties (absolute and relative permeability, porosity, compressibility, initial pressure and initial phase saturations). The produced fluids (light oil, gas, water) are modelled using a black oil simulator. The key question is: can we determine an optimal injection strategy for the oil and gas field?

Figure 8: PIPESIM® multiphase flow model for wellbores and pipelines (CS 1).

Do we maintain a constant flooding/injection rate for the entire production horizon considered (6 years); or is there an optimal way of performing time-dependent water flooding in which injected water rate changes over time, to yield maximum oil production and consequently field profitability?

Figure 9: Reservoir structure showing the fluid regions, drilled and completed wells (CS 1).

Certainly, this is to be done with pivotal concentration on operational constraints such as the size of the surface facilities (separators), available treated water for injection daily, fracture pressure of the reservoir (formation fracture could occur when surface injection pressure supersedes reservoir pressure), wellbore performance hydraulics and operational running costs.

Table 3: Injection and production well properties (CS 1)

The results of streamline simulation generally show good hydraulic injector-producer connection. This is aided by the relatively simple geometry of the reservoir with no isolating fault blocks or other complicating boundaries. In case study 1 (a), A1, A2 and A3 represent the contribution of the injector to the oil production in the 3 producing wells, respectively. PROD_WELL-2 experiences the highest pressure support and thus increased oil production due to injector action (red sector).

Figure 10: Oil production fraction per streamline start point after 365 days (CS 1).

Table 4: Computational summary (CS 1).

We particularly observe in Fig. 10 that, PROD_WELL-3 it is less impacted by the flooding process (illustrated by sector A3 in the pie-chart) compared to the other 2 wells (A1 & A2). B1, B2 and B3 represent production due to other means such as fluid expansion (i.e. as though the injector were absent). This phenomena is due to the complexity of the underlying permeability distribution.

Case Study 2 (CS 2)

This case study involves 4 injection wells and 4 producing wells with some of the wells having deviated geometries. Case 2 maintains a similar concept, with the following modifications vs. Case 1.

Figure 11: PIPESIM® model for the pressure drop determination in wellbores and pipelines (CS).

- Asides the time-dependent allocation problem for a single injector well, another level of complexity arises when we want to know the optimal way to split the injection rates between the various injectors, so that oil production is maximised based on the total available field water. Streamline simulation and injector efficiency calculations are employed again.

Figure 12: Reservoir structure showing the fluid regions, drilled and completed wells (CS 2).

- The network here consists of 2 pipelines that route fluid production from the reservoir to the surface facilities. We do not introduce routing constraints at this stage (which would lead to an MINLP) problem; rather we assume that the 2 horizontal producer wells are connected to the first pipelines and the other 2 vertical wells are connected to the second pipeline.

Table 5: Injection and production well properties (CS 2).

- Field water injection commences at the start of the 3rd production year. At this time, steady production period of respective producer wells has ended and a decline already occurring.

Figure 13: Oil production fraction per streamline start point after 365 days (CS 2).

In case study 2 (b), the colour of the injector well labels correspond to the colours of the respective sectors, which in turn represent the contribution of an injector to the oil flow rate delivered by a particular producer well. For example, water injection from INJ_WELL-2 contributes to the production rates of PROD_WELL-1 (B1) and PROD_WELL-2 (B2) respectively. Both horizontal producers, receive the greatest injection support from INJ_WELL-2; sectors C1 & C2 respectively.

Table 6: Computational summary (CS 2).

Results and Discussion

Optimal injection strategy via simulation and optimisation (CS 1)

Initial averaged results obtained by running the reservoir simulator with injection rates (derived from streamline simulation) are shown in Figs. (14 and 15). Field performance ratios (gas-oil ratio and water cut) and the reservoir pressure are shown in Fig. 14c. The very high GOR values noticed in the Fig. 14a is a strong indicator of how light the oil is and its tendency to form hydrates. As expected, there is a consistent drop in the reservoir pressure with time but to a lesser extent compared to the decline obtainable with a heavy oil. This is attributable to the simultaneous gas production and expansion which provides some pressure support (solution gas drive) in the reservoir. The onset of water injection suppresses the GOR, but conversely increases the field water cut (Fig 14b).

Figure 14: Dynamic reservoir pressure profile and performance ratios, WC and GOR (CS 1).

It is important to ascertain the time-dependent performance of each well in the field. The productivity index (Eq. 1) and injection efficiency are established methods of determining the performance of producer and injector wells, respectively. The rapid increase in productivity index at the start of production occurs due to the high initial reservoir pressure and injection support. The drop in injection efficiency and reservoir pressure are also reflected in the productivity decline of the respective wells. Well 3 is the best performing well; the porosity and permeability distribution around the well is the main factor influencing its performance compared to the other wells. It can also be observed that the injector efficiency computed from the well allocation factors reduces with time and enters a stabilisation zone from 1095 days. This implies that there is a possibility to reduce this injection rate and yet obtain good performance. By exploiting the reservoir's properties, we can find the optimal injection strategy that uses the least injected water, while maintaining/increasing oil production.

Figure 15: Production and injection well performance indicators (CS 1).

The oil, water and gas production profiles and the cumulative production for the respective production wells are shown in Fig. 16. It can be observed that the algorithm was able to determine the oil and gas production decline with time for all wells with PROD_WELL-3 performing best as reflected in the PI. The sharp increase in water production noticed in Fig. 14b occurs when the injector performance is at its best (Fig. 15b); the minimal change in injection efficiency is captured by the algorithm as reflected in the near-stable water production rates (Fig. 16b) after the sharp increase, particularly for PROD_WELL-3 and PROD_WELL-2. We also present a second scenario in which the injection profile is kept constant (at 10000 STB/day) and the production performance of the wells alone is optimised.

Figure 16: Optimal oil, water and gas flowrates from the production wells (CS 1).

The production profiles are compared to the first case in which an optimal injection strategy is sought. We observe that for PROD_WELL-1 and PROD_WELL-2, the oil and gas production rates for the constant injection rates are slightly higher than the optimal injection scenario (Fig. 17a). However, the

Figure 17: Comparison of rate profiles for constant and optimised injection scenarios (CS 1).

optimiser has taken advantage of the productivity of PROD_WELL-3 to enhance the final NPV (Fig. 17a). It is important to mention that this occurs at the expense of water production rate of PROD_WELL-3 (Fig. 17b). There is considerable difference in the water production rates between the optimal and constant injection cases for PROD_WELL-1 and PROD_WELL-2 and PROD_WELL-3, respectively (Fig. 17b). We attribute this to the permeability distribution and the distance between the respective production wells and the injection well; these factors greatly influence the water breakthrough time. Fig. 18 shows the optimal injection strategy as determined by the implemented optimisation framework. At the beginning of production, it can be observed that the optimal injection strategy shows a continuous increase in the injection rate and subsequently a decreased injection rate. It can be deduced that a 30% decrease in the total injected water across the time horizon considered still yields a 1% higher profitability (Fig. 19).

Figure 18: Optimal injection strategy and cumulative injection rates of the field (CS 1).

Calculated voidage replacement ratios (VRR) range between 0.2 and 0.4 for both case scenarios. The VRR is simply the ratio of injected fluid to the reservoir barrels of produced fluid. It determines whether the reservoir pressure is maintained (VRR=1), increased (VRR>1) or experiences a decline (VRR<1) at a particular point in time. The obtained results thus indicate that the reservoir pressure is declining despite the injection of water to the reservoir; more injection wells need to be drilled in order to maintain the reservoir pressure. It also indicates that the obtained production rates are not only due to the injected water volume but also fluid expansion within the reservoir. Also worth mentioning is the fact that optimisation framework adopted here does not only seek to improve the water injection strategy but also the production strategy. Based on the supplied objective function, the algorithm determines if much attention is given to the injection component of the system or the production component while ensuring all constraints are satisfied and the NPV maximised.

Figure 19: NPV analysis for both scenarios (CS 1).

Optimal injection strategy via simulation and optimisation – Case Study 2 (CS 2)

Fig. 20 shows in more detail (compared to Fig. 14) the water cut, GOR and pressure decline for the production wells in the field. The effect of water injection is reflected in the sharp decrease in the

GOR which can be attributed to a reduced gas saturation and increased water mobility in the reservoir. The GOR for wells however picks up over time except that of PROD_WELL-3 which is the least affected by the water injection process. This behaviour can be further understood by examining the water cut profile. The relative increment in the water cut at the start of water injection supersedes other wells. PROD_WELL-1 and PROD_WELL-2 have very similar performance ratios. Fig. 20b shows that water production in these wells does not commence until the 365th day of production, indicating they are strategically positioned to reduce the negative effects of possible water conning.

Figure 20: Dynamic reservoir pressure profile and performance ratios (water cut and GOR) (CS 2).

In order to demonstrate the extent of pressure support in the field, a plot of the reservoir pressure with and without water injection is shown in Fig. 20c. It is clearly demonstrated that the rate of pressure decline is faster when water injection is neglected. Without increased production time, this could reduce further below the bubble point, thus triggering increased gas production.

The productivity indices and injector efficiencies of the production and injection wells are shown in Fig. 21b. We observe that PROD_WELL-1 slightly outperforms PROD_WELL-2; their equidistant locations from the INJ_WELL-1 and similarity in the permeability distribution around them implies they experience similar levels of contribution from the injection well (Fig. 13). Also observed, is the reduced productivity of the vertical wells (PROD_WELL-3 and PROD_WELL-4) compared to the horizontal wells (PROD_WELL-1 and PROD_WELL-2). This is inevitably due to the higher drainage area the horizontal wells are exposed to in the reservoir (Fig. 21a). The huge disparity observed in the well productivity profiles is not the case with the streamline-derived injection efficiencies (Fig. 21b). Despite the favourable well geometry of INJ_WELL-2 (horizontal) compared to INJ_WELL-4 (vertical), they both exhibit similar efficiencies. The interaction of INJ_WELL-1 with the horizontal producers is the main factor contributing to its high efficiencies as indicated by the well allocation factors obtained from streamline simulation. With the daily available field water injection rate of 75,000 STB/day, it was possible to propose initial injection rates to the optimization algorithm.

Figure 21: Production and injection well performance indicators (CS 2).

The production rate profiles for the oil, gas and water phase of the respective production wells are presented in Fig. 22. Based on the production data supplied and the proxy modelling techniques adopted, the algorithm captures the increment in oil production at the start of injection and the reduction in the decline rate (Fig. 22a). The water production rates observed are well representative of the water cut profiles obtained from the reservoir simulator in Fig. 20b, with the 2 horizontal producers, yielding lower water production rates compared to the vertical producers. Just like the oil production rate profile, the gas production rates of the respective wells also shows an increment in production due to water injection and this is more significant for the horizontal wells.

Figure 22: Optimal oil, water and gas flowrates from the production wells (CS 2).

In the second scenario in which the injection rate is maintained at the maximum allowable rate for each injection well, we observe that the superior performance of the horizontal wells has been exploited by the optimisation algorithm for the improvement in in the total oil production (Fig. 23a). This was similarly observed in case study 1, in which PROD_WELL-3 had the highest contribution to the difference in NPV noticed for the 2 scenarios. For the other vertical producers, there is no difference between the observed production rates for the optimal and constant injection scenarios. The optimal injection strategy and the corresponding cumulative injection rate for each well are shown in Fig. 24. It is illustrated that a step wise increase in the injection rate for INJ_WELL-1 and a constant injection the rest of the wells is guaranteed is increase the NPV of the field by 6% (Fig. 25) and also reduce the total water consumption by 11%.

Figure 23: Comparison of rate profiles for the constant and optimised injection scenarios (CS 2).

The drilling of 1 new producer well and 3 more injector wells in case study 2, resulted in the increase of the VRR to a range of 0.25 – 0.5 for the optimal and constant injection scenarios.

Figure 24: Injection rates for optimal (a & c) and constant injection scenarios (b & d) – (CS 2).

As explained in case study 1, more recovery mechanisms are activated when VRR<1 compared to a VRR of 1. Complementing the water injection process with some other production enhancement mechanism may lead to increased oil production. Although more water can be injected to increase the

VRR considerably, the field engineer must ensure that this is not at the expense of the field water cut, which if too high could create a new set of operational problems.

Figure 25: NPV analysis for both scenarios (CS 2).

Solver performance and scaling

Different types of algorithms have been implemented on a wide variety of production optimization problems and this is dependent on the characteristics of the objective function and constraints. Local searching methods equipped with quadratic proxy models and many reasonable initial guesses are able to exploit smooth features of the objective function, and converge rapidly to a global optimum. Majority of the computational effort involved in solving problems with discrete variables can be attributed to the piecewise linearization procedure and the number of breakpoints required to capture nonlinearities in well and pipeline models.[5] The absence of these variable types in our case studies grossly reduces the computational effort as reflected in Table 7 compared to the MILP/MINLP studies. Although the proposed optimisation formulation is not guaranteed to find a global optimal solution, a useful feasible solution is found within a very short duration; this demonstrates its applicability as a viable tool during oilfield planning and operation.

Short solution times observed (Table 7) can be attributed to a reduced simulator search time in the respective component simulators. This is obtained without the parallelization of the different component simulators or the optimisation algorithm adopted. This facilitates real time application of the results for supporting operational decisions. The parallelisation adopted here was to assign the running of the optimisation algorithm for the 1000 initial guesses to the different processing cores. With the implemented parallel computing procedure and the convergence speed for each set of initial guesses, running the algorithm several times proved attractive. The average variation across all initial starting points was 5%; thus proving the robustness of the problem structure formulation. It is also possible to attribute this value to the efforts put in place via sophisticated reservoir simulation to ensure that the perturbation of the initial guesses were between operationally feasible bounds. It should be noted that with an increase in problem size (production system components), comes a rapid

increase in the number of variables and thus an increase in the solution times. The structural breakdown of the network also implies, more proxy model evaluations at the different periods would be necessary. Considerable presolving effort is required for multiperiod proxy model generation.

Furthermore, an important aspect of the multiperiod proxy modelling technique adopted here is the fact that abrupt changes in multiphase flow behaviour can be easily incorporated. However, we avoid these sudden changes in pipeline conditions by ensuring that the operational pressure and temperature in the pipeline are outside the hydrate formation region. If such conditions exist, it is possible to have discontinuities in the pressure-rate response of the pipeline. This in turn affects the accuracy of the relatively straight forward quadratic polynomial proxy model and also the accuracy and applicability of the optimisation results. In cases where such abrupt flow regime changes cannot be avoided, cubic spline interpolation may serve as a more sophisticated tool for capturing the nonlinearities.

Although we have assumed a 1 year interval update in our case studies, this is specific to the nature of the reservoir dynamic behaviour. It is expected that a more frequent update of the reservoir properties in the optimisation formulation yields more accurate results; however, we have chosen this time frame in such a way that the overall reservoir properties' dynamic trend is still honoured (via time averaging analysis for the PI, WC and GOR respectively). This was possible because of the relatively simple geometry of the reservoir and the permeability distribution. It is thus worth noting that a satisfactory trade-off has to be made between the model formulation time (by applying smaller time discretisation) and its quality/accuracy. Although the application of GA yielded only a marginal improvement in proxy model accuracy attained via least squares regression, mean errors obtained by comparing simulator data and proxy model data were less than 2%. Ensuring that simulation results are history-matched to real field data is an important step but can only be done if data is available. Although, no field data was used in this case study, synthetic data adopted are well representative of practical conditions obtainable during field operations. The disparity in the magnitude of the different variables has to be reduced by adopting systematic scaling methods in order to ensure good performance of the optimisation solvers (prescribed tolerances and other stopping criteria in an unscaled NLP problem

may cause convergence difficulties). Thus we particularly ensured that each constraint (especially those for gas flow rates) is well-conditioned with respect to other variable perturbations.

Table 7: Solver performance analysis.

A comparison of the solvers' performance is shown in Table 7 and Fig. 26. In case study 1, it is observed that the IPOPT solver converges to a higher NPV than the MATLAB's fmincon solver. Although similar production profiles were obtained using the MATLAB fmincon solver, they are not presented here because fmincon failed to satisfy all constraints within the acceptable tolerance.

Figure 26: Solver performance for constant and optimised injection scenarios (CS 1: a, CS 2: b).

Furthermore, in case study 2, the MATLAB fmincon solver was unable to yield satisfactory results that met the convergence criteria; hence its function evaluation history is also not presented. It is also worth mentioning that the highest NPV from the 1000 initial guesses supplied and the corresponding parameters for that NPV value was chosen as the optimal parameter set.

Conclusions

In this work we have simultaneously addressed a production and injection optimisation problem with an economic objective function in terms of the Net Present Value (NPV) subject to practical constraints that ensure operational feasibility. Also demonstrated in this paper is the multifaceted nature of a petroleum production system that allows its components to be treated independently; however with an objective function that comprehensively captures individual component characteristics. On the basis of the computations performed, we derive the following conclusions:

- The application of streamline-based well allocation factors and injector efficiency is a reliable method of obtaining good initial guesses for the time-dependent injection rates. Furthermore, the sensitivity of the optimiser to the supplied initial guesses can be reduced by perturbing sound initial guesses with reasonable bounds; thus yielding a near-global solution.
- High resolution data tables obtained via numerous simulation runs and quadratic proxy modelling are very useful tools for approximating nonlinear system behaviour, providing an excellent platform for the application of gradient-based optimisation methods.

- Although it is usually expected that an increased water injection rate yields a higher oil sweep efficiency, the underlying permeability distribution and other reservoir properties could complicate this expectation. Our developed optimisation framework has shown that a systematic variation of the injection rates, well head pressures and production rates yields increased field profitability. In our considered case study 1, a slightly improved NPV (1%) is achievable with an optimal injection strategy which decreases field water consumption by 30%. Implementing a similar strategy on the second case study yields 6% improvement in the NPV and a corresponding 11% decrease in the total field water consumption.

- The IPOPT solver showed superior performance to the MATLAB fmincon solver with respect to number of iterations and simulation time, a difference accentuated by increased problem size and complexity. However, considering the limitations of the two-phase IPOPT algorithm, in which the feasibility restoration phase may fail when called, algorithmic modifications (e.g. one-phase interior point method [57]) can be pursued. Our effort coincides with software developments which foster interoperability between proprietary system simulation suites and open-source optimisation solvers, [58] paving the way for new advances.

The water flooding optimisation approach [49] is a heuristic reservoir engineering-driven method that does not guarantee optimality. Nevertheless, the simulation-based optimisation approach proposed in the present paper is a definite improvement in the state of the art, integrating the concepts of reservoir simulation and surface facility optimisation, to ensure a more robust and optimal operating strategy.

Acknowledgements

The authors gratefully acknowledge the financial support of the University of Edinburgh via a School of Engineering PhD scholarship awarded to Mr E. I. Epelle. Moreover, Dr D. I. Gerogiorgis acknowledges a Royal Academy of Engineering (RAEng) Industrial Fellowship. Tabulated and cited literature data suffice for reproduction of all original simulation results and no other supporting data are required to ensure reproducibility.

Literature References

1. Gunnerud V, Conn A, Foss B. Embedding structural information in simulation-based optimization. *Computers & Chemical Engineering*. 2013;53:35-43.
2. Tavallali MS, Karimi IA, Teo KM, Baxendale D, Ayatollahi S. Optimal producer well placement and production planning in an oil reservoir. *Computers & Chemical Engineering*. 2013;55:109-125.
3. Epelle EI, Gerogiorgis DI. A multiparametric CFD analysis of multiphase annular flows for oil and gas drilling applications. *Computers & Chemical Engineering*. 2017;106:645-661.
4. Epelle EI, Gerogiorgis DI. Transient and steady state analysis of drill cuttings transport phenomena under turbulent conditions. *Chemical Engineering Research and Design*. 2018a;131:520-544.
5. Epelle EI, Gerogiorgis DI. CFD modelling and simulation of drill cuttings transport efficiency in annular bends: Effect of particle sphericity. *Journal of Petroleum Science and Engineering*. 2018b;170:992-1004.
6. Kosmidis VD, Perkins JD, Pistikopoulos EN. Optimization of well oil rate allocations in petroleum fields. *Industrial & Engineering Chemistry Research*. 2004;43(14):3513-3527.
7. Kosmidis VD, Perkins JD, Pistikopoulos EN. A mixed integer optimization formulation for the well scheduling problem on petroleum fields. *Computers & Chemical Engineering*. 2005;29(7):1523-1541.
8. Bailey B, Crabtree M, Tyrie J, Elphick J, Kuchuk F, Romano C, Roodhart L. Water control. *Oilfield Review*. 2000;12(1):30-51.
9. Barragán-Hernández V, Vázquez-Román R, Rosales-Marines L, García-Sánchez F. A strategy for simulation and optimization of gas and oil production. *Computers & Chemical Engineering*. 2005;30(2):215-227.
10. Nikolaou M, Cullick AS, Saputelli LA. Production optimization: A moving-horizon approach. *In Society of Petroleum Engineers-SPE Intelligent Energy Conference and Exhibition*. 2006a;1-13.
11. Nikolaou M, Cullick AS, Saputelli LA, Mijares G, Sankaran S, Reis LC. A consistent approach towards reservoir simulation at different time scales. *In Society of Petroleum Engineers-SPE Intelligent Energy Conference and Exhibition*. 2006b;1-9.
12. Awasthi A, Sankaran S, Nikolaou M, Saputelli L, Mijares G. Closing the gap between reservoir modeling and production optimization. *In Society of Petroleum Engineers-SPE Digital Energy Conference and Exhibition.* 2007;1-20.

13. Awasthi A, Nikolaou M, Saputelli LA, Mijares G. Meeting the challenges of real-time production optimization – A parametric model-based approach. *In Society of Petroleum Engineers-SPE Intelligent Energy Conference and Exhibition.* 2008a;1-18.
14. Awasthi A, Sankaran S, Nikolaou M, Saputelli L, Mijares G. Short-term production optimization by automated adaptive modeling and control. *In Society of Petroleum Engineers-SPE Intelligent Energy Conference and Exhibition*. 2008b;1-16.
15. Gunnerud V, Foss B. Oil production optimization—A piecewise linear model, solved with two decomposition strategies. *Computers & Chemical Engineering*. 2010;34(11):1803-1812.
16. Gunnerud V, Foss BA, McKinnon KI, Nygreen B. Oil production optimization solved by piecewise linearization in a Branch & Price framework. *Computers & Operations Research*. 2012;39(11):2469-2477.
17. Silva TL, Camponogara E. A computational analysis of multidimensional piecewise-linear models with applications to oil production optimization. *European Journal of Operational Research*. 2014;232(3):630-642.
18. Codas A, Campos S, Camponogara E, Gunnerud V, Sunjerga S. Integrated production optimization of oil fields with pressure and routing constraints: The Urucu field. *Computers & Chemical Engineering*. 2012;46:178-189.
19. Tavallali MS, Karimi IA, Halim A, Baxendale D, Teo KM. Well placement, infrastructure design, facility allocation, and production planning in multireservoir oil fields with surface facility networks. *Industrial & Engineering Chemistry Research*. 2014;53(27):11033-11049.
20. Tavallali MS, Karimi IA. Integrated oil-field management: from well placement and planning to production scheduling. *Industrial & Engineering Chemistry Research*. 2016;55(4):978-994.
21. Tavallali MS, Karimi IA, Baxendale D. Process systems engineering perspective on the planning and development of oil fields. *AIChE Journal*. 2016;62(8):2586-2604.
22. Duran MA, Grossmann IE. An outer-approximation algorithm for a class of mixed-integer nonlinear programs. *Mathematical Programming.* 1986;36(3):307-339.
23. Kocis GR, Grossmann IE. A modelling and decomposition strategy for the MINLP optimization of process flowsheets. *Computers & Chemical Engineering*. 1989;13(7):797-819.
24. Viswanathan J, Grossmann IE. A combined penalty function and outer-approximation method for MINLP optimization. *Computers & Chemical Engineering*. 1990;14(7):769-782.

25. Iyer RR, Grossmann IE, Vasantharajan S, Cullick AS. Optimal planning and scheduling of offshore oil field infrastructure investment and operations. *Industrial & Engineering Chemistry Research*. 1998;37(4):1380-1397.
26. van den Heever SA, Grossmann IE. An iterative aggregation/disaggregation approach for the solution of a mixed-integer nonlinear oilfield infrastructure planning model. *Industrial & Engineering Chemistry Research*. 2000;39(6):1955-1971.
27. van den Heever SA, Grossmann IE, Vasantharajan S, Edwards K. Integrating complex economic objectives with the design and planning of offshore oilfield infrastructures. *Computers & Chemical Engineering*. 2000;24(2-7):1049-1055.
28. van den Heever SA, Grossmann IE, Vasantharajan S, Edwards K. A Lagrangean decomposition heuristic for the design and planning of offshore hydrocarbon field infrastructures with complex economic objectives. *Industrial & Engineering Chemistry Research*. 2001;40(13):2857-2875.
29. Gupta V, Grossmann IE. An efficient multiperiod MINLP model for optimal planning of offshore oil and gas field infrastructure. *Industrial & Engineering Chemistry Research*. 2012;51(19):6823-6840.
30. Gupta V, Grossmann IE. Modeling and computational strategies for optimal development planning of offshore oilfields under complex fiscal rules. *Industrial & Engineering Chemistry Research*. 2012;51(44):14438-14460.
31. Bellout MC, Ciaurri DE, Durlofsky LJ, Foss B, Kleppe J. Joint optimization of oil well placement and controls. Computational Geosciences. 2012;16(4):1061-1079.
32. Li L, Jafarpour B, Mohammad-Khaninezhad MR. A simultaneous perturbation stochastic approximation algorithm for coupled well placement and control optimization under geologic uncertainty. *Computational Geosciences*. 2013;17(1):167-188.
33. Azamipour V, Assareh M, Dehghani MR, Mittermeir GM. An efficient workflow for production allocation during water flooding. *Journal of Energy Resources Technology*. 2017;139(3):1-10.
34. Azamipour V, Assareh M, Mittermeir GM. An improved optimization procedure for production and injection scheduling using a hybrid genetic algorithm. *Chemical Engineering Research and Design*. 2018;131:557-570.
35. Gerogiorgis DI, Georgiadis M, Bowen G, Pantelides CC, Pistikopoulos EN. Dynamic oil and gas production optimization via explicit reservoir simulation. *Computer Aided Chemical Engineering*. 2006;21:179-184.

36. Gerogiorgis DI, Kosmidis VD, Pistikopoulos EN. Mixed Integer Optimization in Well Scheduling. *Encyclopedia of Optimization*. 2009;2247-2270.
37. Fujita Y, Datta-Gupta A, King MJ. A comprehensive reservoir simulator for unconventional reservoirs that is based on the Fast Marching method and diffusive time of flight. *SPE Journal.* 2016;21(06):2-76.
38. Taware S, Alhuthali AH, Sharma M, Datta-Gupta A. Optimal rate control under geologic uncertainty: water flood and EOR processes. *Optimization and Engineering.* 2017;18(1):63-86.
39. Liu S, Valkó PP. Optimization of spacing and penetration ratio for infinite-conductivity fractures in unconventional reservoirs: A section-based approach. *SPE Journal*. 2017;1-16.
40. Narasingam A, Kwon JS. Development of local dynamic mode decomposition with control: Application to model predictive control of hydraulic fracturing. *Computers & Chemical Engineering*. 2017;106:501-511.
41. Siddhamshetty P, Yang S, Kwon JS. Modeling of hydraulic fracturing and designing of online pumping schedules to achieve uniform proppant concentration in conventional oil reservoirs. *Computers & Chemical Engineering*. 2018;114:306-317.
42. Siddhamshetty P, Kwon JS, Liu S, Valkó PP. Feedback control of proppant bank heights during hydraulic fracturing for enhanced productivity in shale formations. *AIChE Journal*. 2018;64(5):1638-1650.
43. Narasingam A, Siddhamshetty P, Sang-Il Kwon J. Temporal clustering for order reduction of nonlinear parabolic PDE systems with time-dependent spatial domains: Application to a hydraulic fracturing process. *AIChE Journal*. 2017;63(9):3818-3831.
44. Narasingam A, Kwon JS. Data-driven identification of interpretable reduced-order models using sparse regression. *Computers & Chemical Engineering*. 2018;119:101-111.
45. Joshi SD. *Horizontal Well Technology.* PennWell Books (Houston, TX, USA); 1991.
46. Schlumberger, *PETREL® Training Manual*. Schlumberger Ltd. (Houston, TX, USA). 2017.
47. Schlumberger, *ECLIPSE® User Manual*. Schlumberger Ltd. (Houston, TX, USA). 2017.
48. Schlumberger, *FrontSIM® User Guide,Technical Description.* Schlumberger Ltd. (Houston, TX, USA). 2017.
49. Thiele MR, Batycky RP. Using streamline-derived injection efficiencies for improved waterflood management. *SPE Reservoir Evaluation & Engineering*. 2006;9(02):187-196.

50. Zangl G, Graf T, Al-Kinani A. Proxy modeling in production optimization. *In Society of Petroleum Engineers-SPE Europec/EAGE Annual Conference and Exhibition*. 2006;1-7.
51. Yeten B, Castellini A, Guyaguler B, Chen WH. A comparison study on experimental design and response surface methodologies. *In Society of Petroleum Engineers-SPE Reservoir Simulation Symposium*. 2005;1-15
52. Schlumberger, *PIPESIM® User Manual*. Schlumberger Ltd. (Houston, TX, USA). 2017.
53. Wächter A, Biegler LT. Line search filter methods for nonlinear programming: Motivation and global convergence. *SIAM Journal on Optimization*. 2005;16(1):1-31.
54. Wächter A, Biegler LT. On the implementation of an interior-point filter line-search algorithm for large-scale nonlinear programming. *Mathematical Programming*. 2006;106(1):25-57.
55. Nocedal J, Wächter A, Waltz RA. Adaptive barrier update strategies for nonlinear interior methods. *SIAM Journal on Optimization*. 2009;19(4):1674-1693.
56. Nocedal J, Öztoprak F, Waltz RA. An interior point method for nonlinear programming with infeasibility detection capabilities. *Optimization Methods and Software*. 2014;29(4):837-54.
57. Hinder O, Ye Y. A one-phase interior point method for nonconvex optimization (Stanford University). *arXiv preprint* arXiv:1801.03072. 2018;1-30.
58. Currie J, Wilson DI, Sahinidis N, Pinto J. OPTI: lowering the barrier between open source optimizers and the industrial MATLAB user. *Foundations of Computer-Aided Process Operations*. 2012;24:32-38.

LIST OF FIGURE CAPTIONS

FIGURE 1

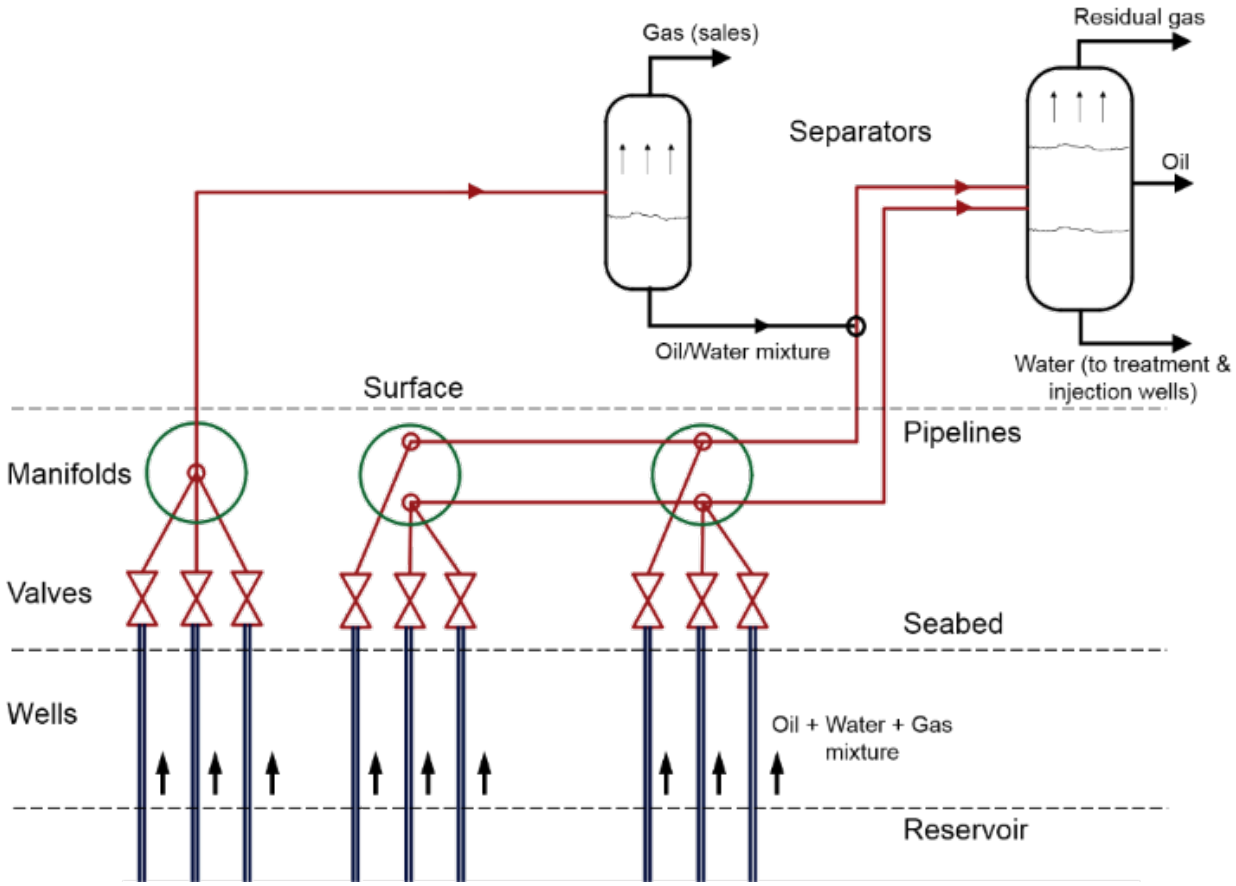
Gas (sales)
Residual gas
Separators
Oil
Oil/Water mixture
Water (to treatment & injection wells)
Surface
Pipelines
Manifolds
Valves
Seabed
Wells
Oil + Water + Gas mixture
Reservoir

FIGURE 2

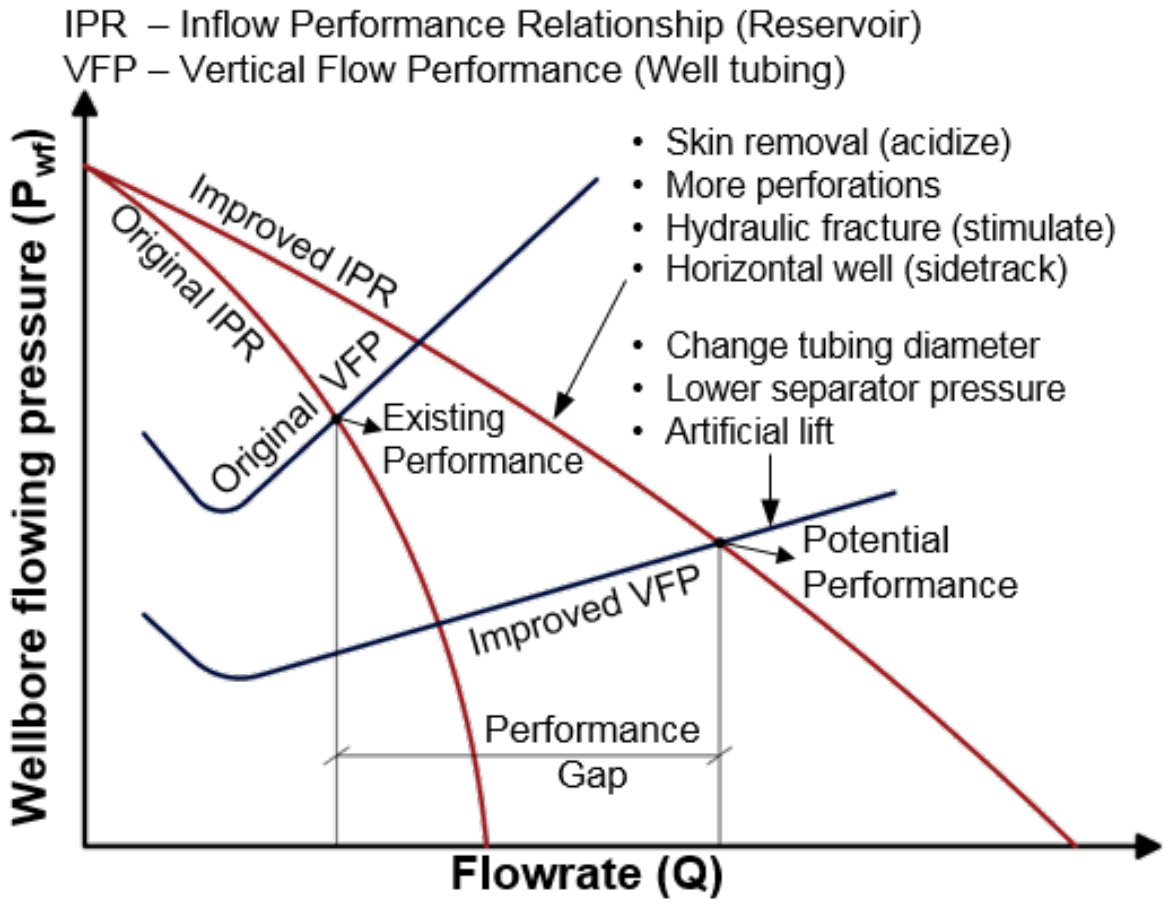
IPR – Inflow Performance Relationship (Reservoir)
VFP – Vertical Flow Performance (Well tubing)
Wellbore flowing pressure (P_{wf})
Flowrate (Q)
Improved IPR
Original IPR
Original VFP
Existing Performance
Improved VFP
Potential Performance
Performance Gap
• Skin removal (acidize)
• More perforations
• Hydraulic fracture (stimulate)
• Horizontal well (sidetrack)
• Change tubing diameter
• Lower separator pressure
• Artificial lift

FIGURE 3

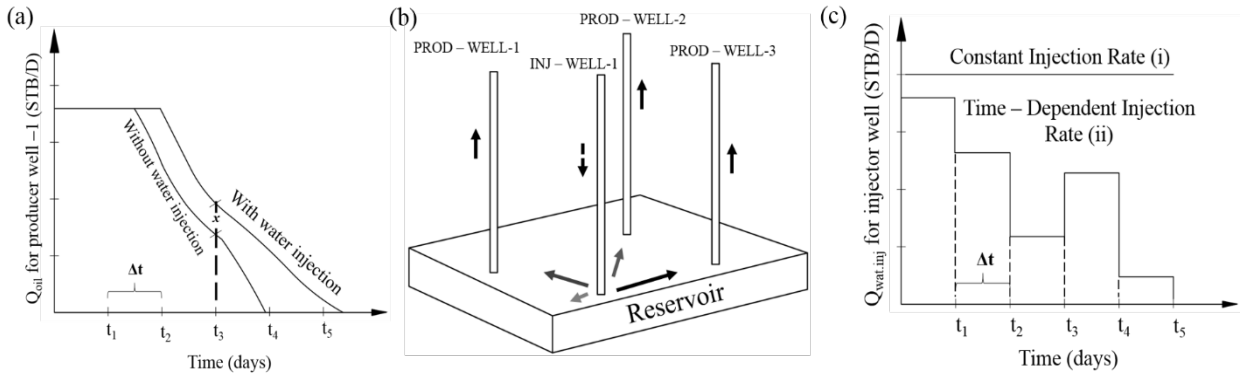
(a)
Q_{oil} for producer well –1 (STB/D)
Without water injection
With water injection
Δt
t_1 t_2 t_3 t_4 t_5
Time (days)
(b)
PROD – WELL-2
PROD – WELL-1
INJ – WELL-1
PROD – WELL-3
Reservoir
(c)
$Q_{wat.inj}$ for injector well (STB/D)
Constant Injection Rate (i)
Time – Dependent Injection Rate (ii)
Δt
t_1 t_2 t_3 t_4 t_5
Time (days)

FIGURE 4

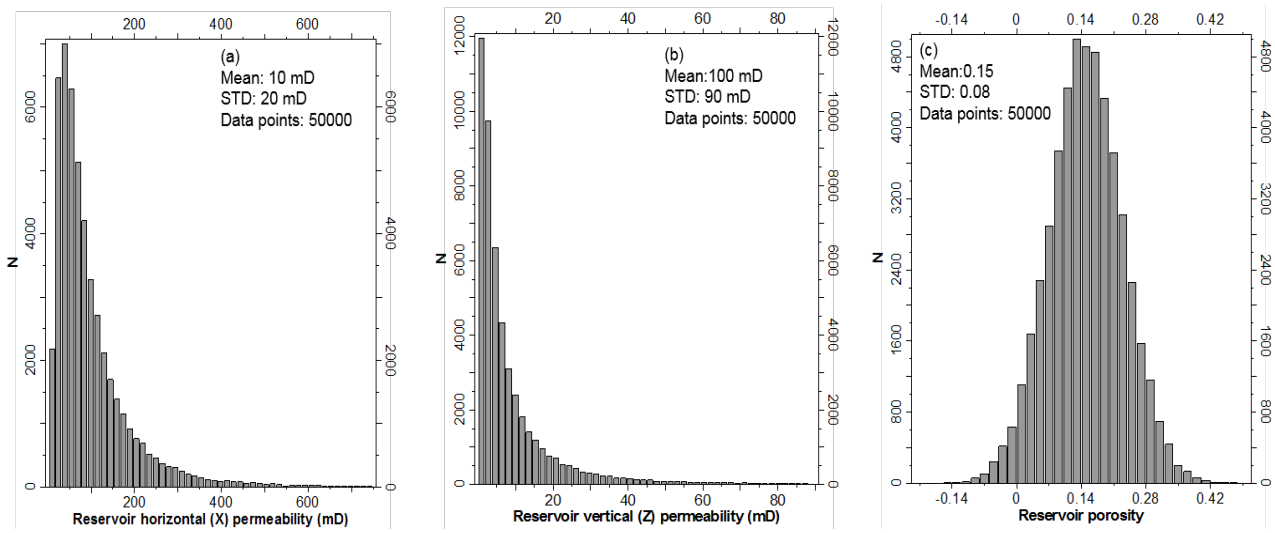
(a)
Mean: 10 mD
STD: 20 mD
Data points: 50000
N
Reservoir horizontal (X) permeability (mD)
(b)
Mean:100 mD
STD: 90 mD
Data points: 50000
N
Reservoir vertical (Z) permeability (mD)
(c)
Mean:0.15
STD: 0.08
Data points: 50000
N
Reservoir porosity

FIGURE 5

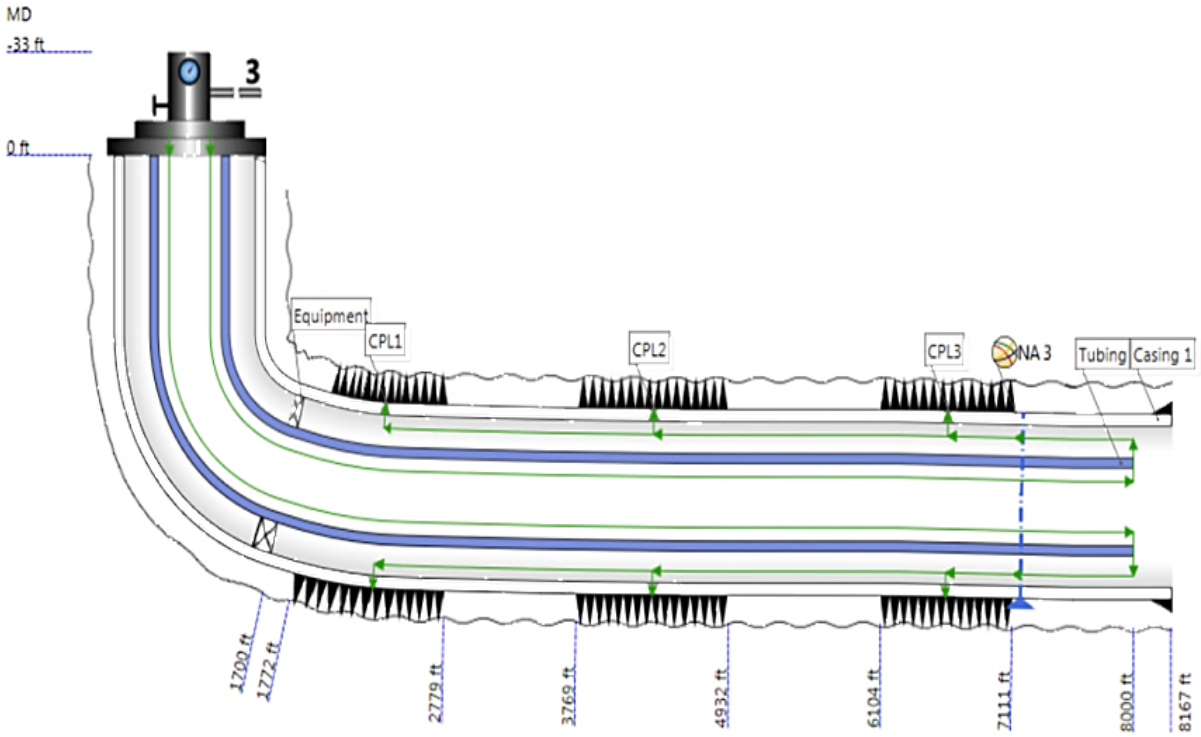
MD
-33 ft
0 ft
3
Equipment
CPL1
CPL2
CPL3
NA 3
Tubing
Casing 1
1700 ft
1772 ft
2779 ft
3769 ft
4932 ft
6104 ft
7111 ft
8000 ft
8167 ft

FIGURE 6

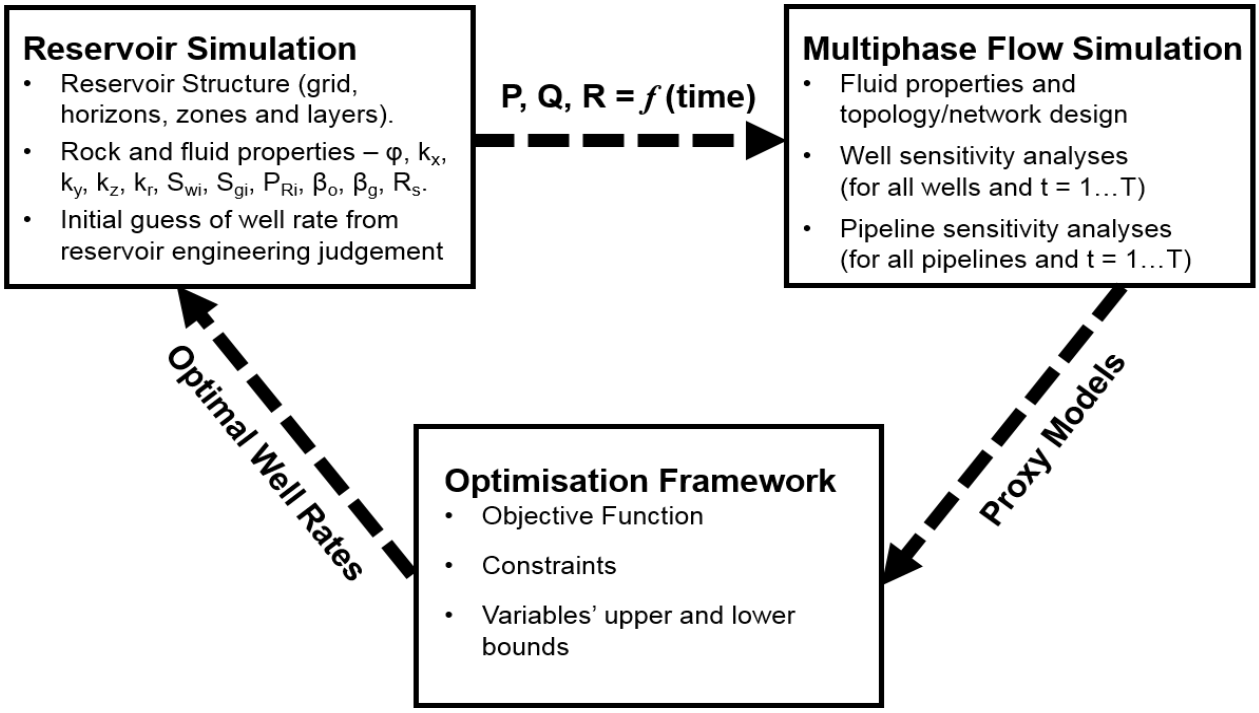
Reservoir Simulation
• Reservoir Structure (grid, horizons, zones and layers).
• Rock and fluid properties – φ, k_x, k_y, k_z, k_r, S_{wi}, S_{gi}, P_{Ri}, β_o, β_g, R_s.
• Initial guess of well rate from reservoir engineering judgement
P, Q, R = f (time)
Multiphase Flow Simulation
• Fluid properties and topology/network design
• Well sensitivity analyses (for all wells and t = 1…T)
• Pipeline sensitivity analyses (for all pipelines and t = 1…T)
Optimal Well Rates
Proxy Models
Optimisation Framework
• Objective Function
• Constraints
• Variables' upper and lower bounds

FIGURE 7

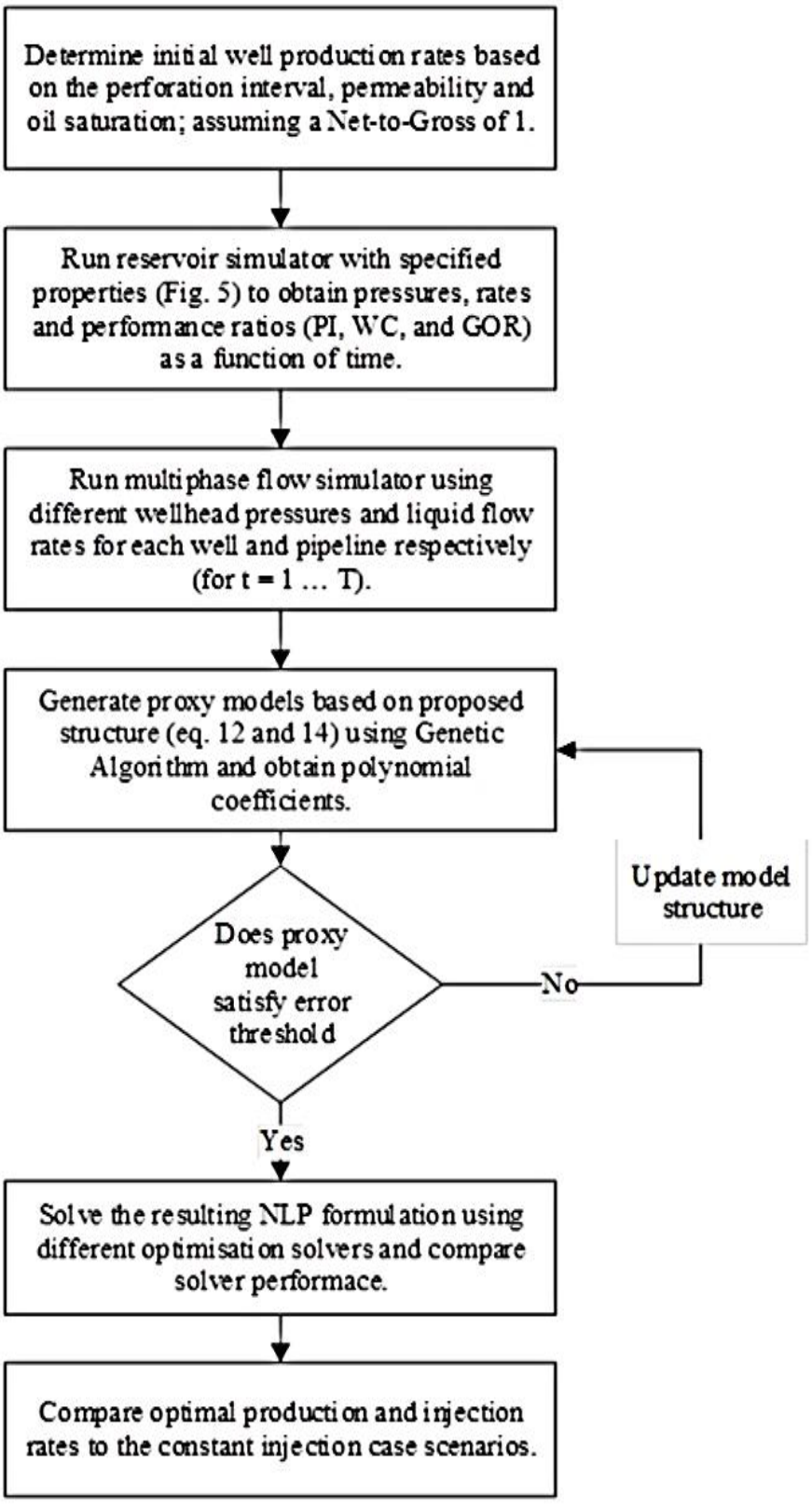
Determine initial well production rates based on the perforation interval, permeability and oil saturation; assuming a Net-to-Gross of 1.
Run reservoir simulator with specified properties (Fig. 5) to obtain pressures, rates and performance ratios (PI, WC, and GOR) as a function of time.
Run multiphase flow simulator using different wellhead pressures and liquid flow rates for each well and pipeline respectively (for t = 1 … T).
Generate proxy models based on proposed structure (eq. 12 and 14) using Genetic Algorithm and obtain polynomial coefficients.
Does proxy model satisfy error threshold
No
Update model structure
Yes
Solve the resulting NLP formulation using different optimisation solvers and compare solver performace.
Compare optimal production and injection rates to the constant injection case scenarios.

FIGURE 8

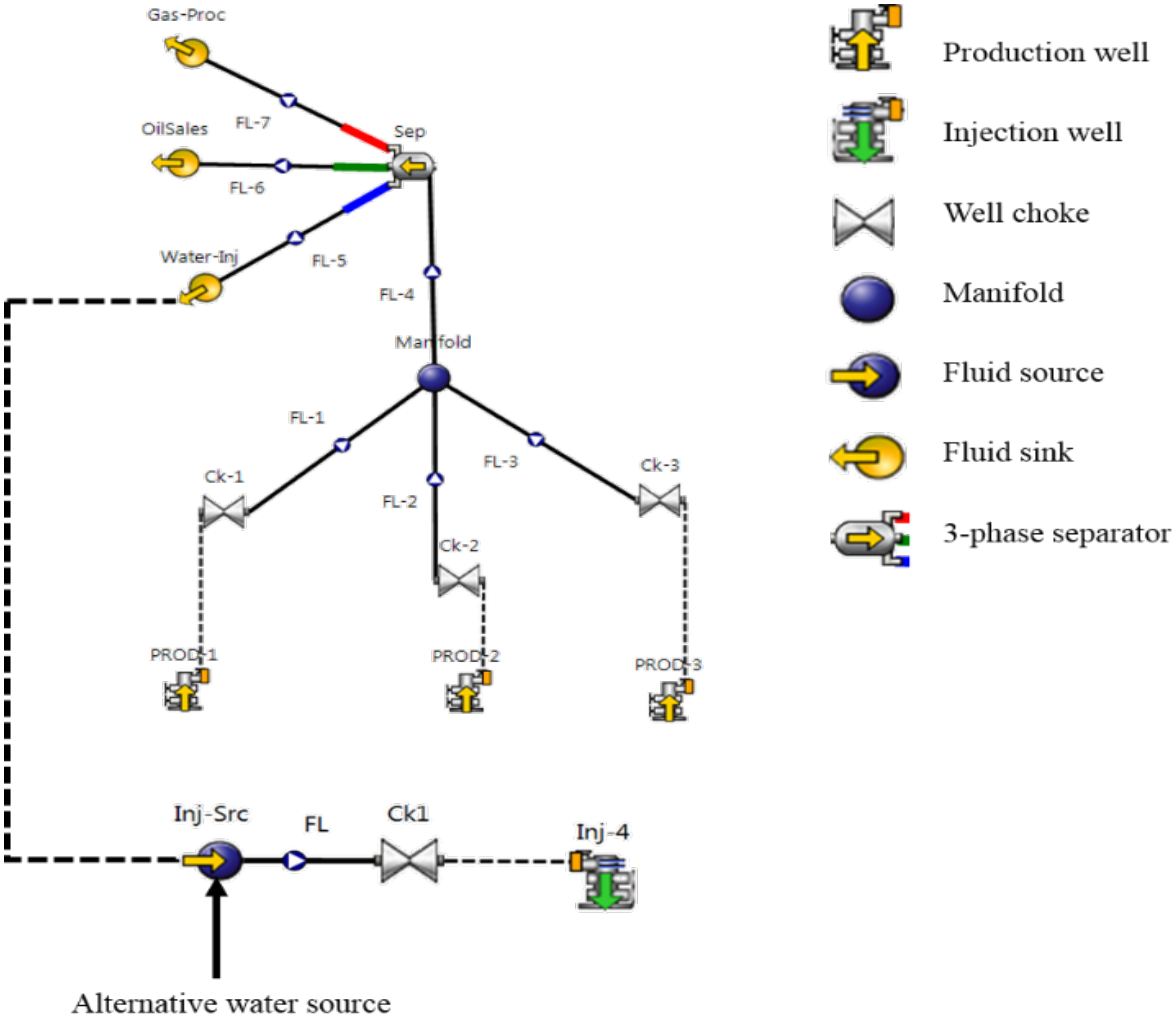
Gas-Proc
OilSales
FL-7
Sep
FL-6
Water-Inj
FL-5
FL-4
Manifold
FL-1
FL-3
Ck-1
FL-2
Ck-3
Ck-2
PROD-1
PROD-2
PROD-3
Inj-Src
FL
Ck1
Inj-4
Alternative water source
Production well
Injection well
Well choke
Manifold
Fluid source
Fluid sink
3-phase separator

FIGURE 9

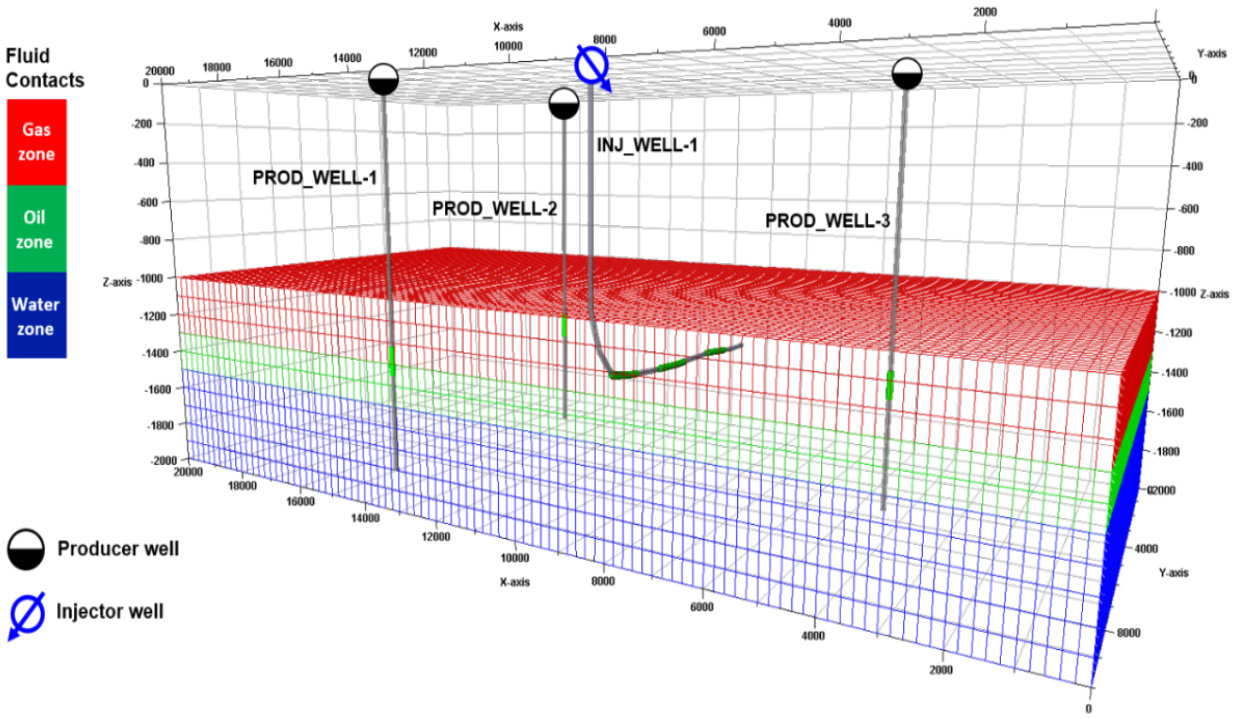
Fluid Contacts
Gas zone
Oil zone
Water zone
Producer well
Injector well
PROD_WELL-1
PROD_WELL-2
INJ_WELL-1
PROD_WELL-3
X-axis
Y-axis
Z-axis

FIGURE 10

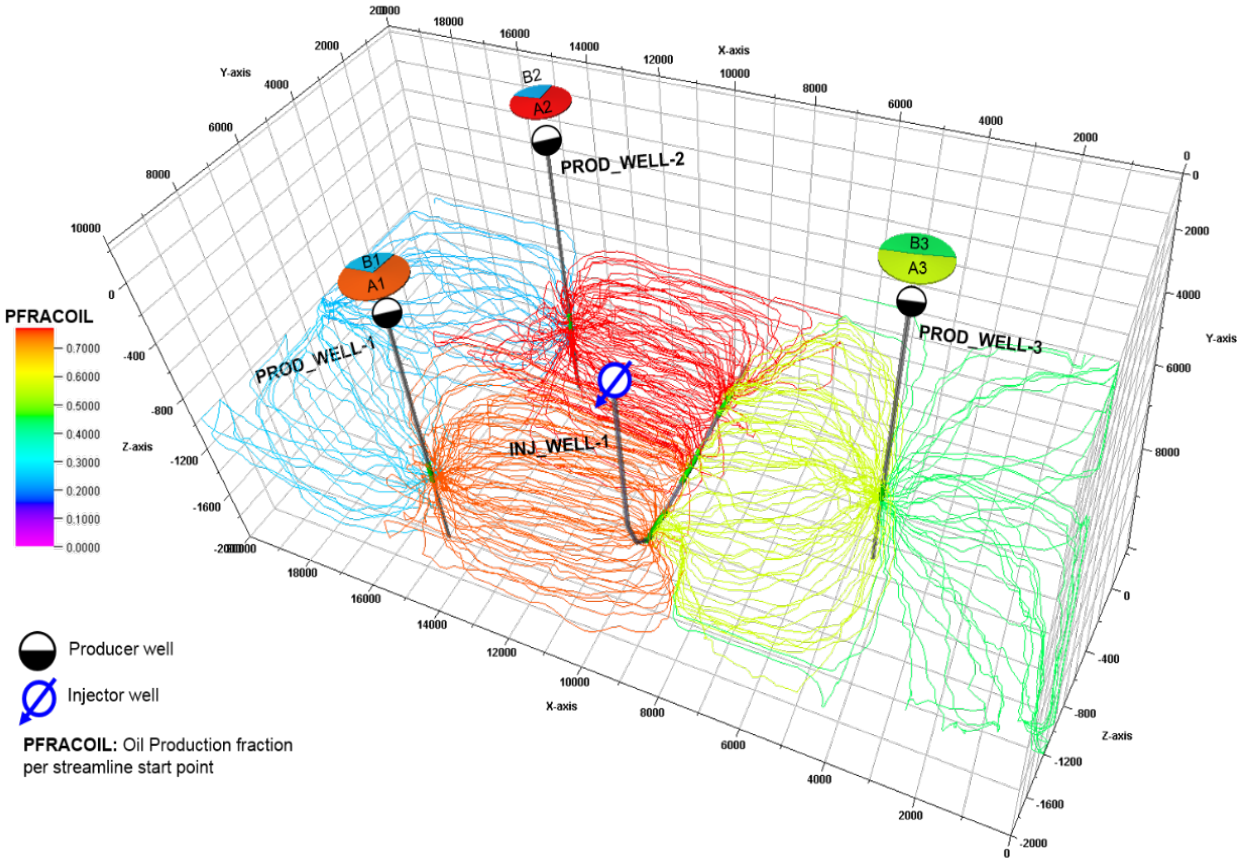
PFRACOIL
0.7000
0.6000
0.5000
0.4000
0.3000
0.2000
0.1000
0.0000
PROD_WELL-1
PROD_WELL-2
PROD_WELL-3
INJ_WELL-1
B1
A1
B2
A2
B3
A3
X-axis
Y-axis
Z-axis
Producer well
Injector well
PFRACOIL: Oil Production fraction per streamline start point

FIGURE 11

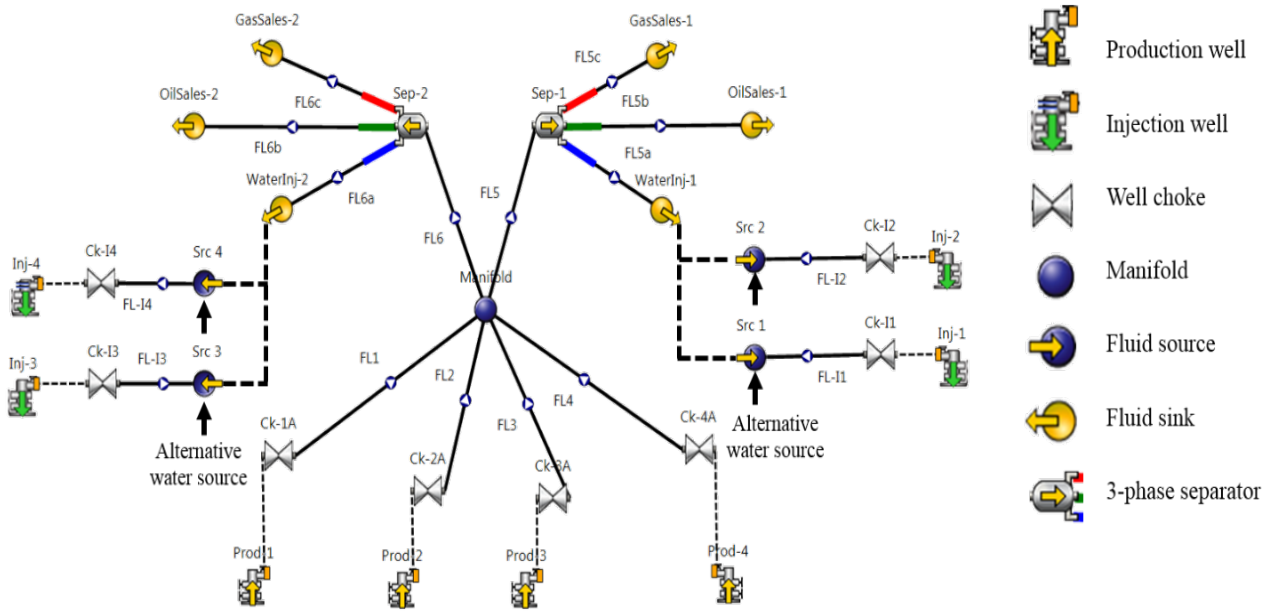
GasSales-2
GasSales-1
FL5c
OilSales-2
FL6c
Sep-2
Sep-1
FL5b
OilSales-1
FL6b
FL5a
WaterInj-2
FL6a
FL5
WaterInj-1
FL6
Src 2
Ck-I2
Inj-2
Inj-4
Ck-I4
Src 4
Manifold
FL-I2
FL-I4
Src 1
Ck-I1
Inj-1
Inj-3
Ck-I3
FL-I3
Src 3
FL1
FL2
FL4
FL-I1
Ck-1A
FL3
Ck-4A
Alternative
water source
Alternative
water source
Ck-2A
Ck-3A
Prod-1
Prod-2
Prod-3
Prod-4
Production well
Injection well
Well choke
Manifold
Fluid source
Fluid sink
3-phase separator

FIGURE 12

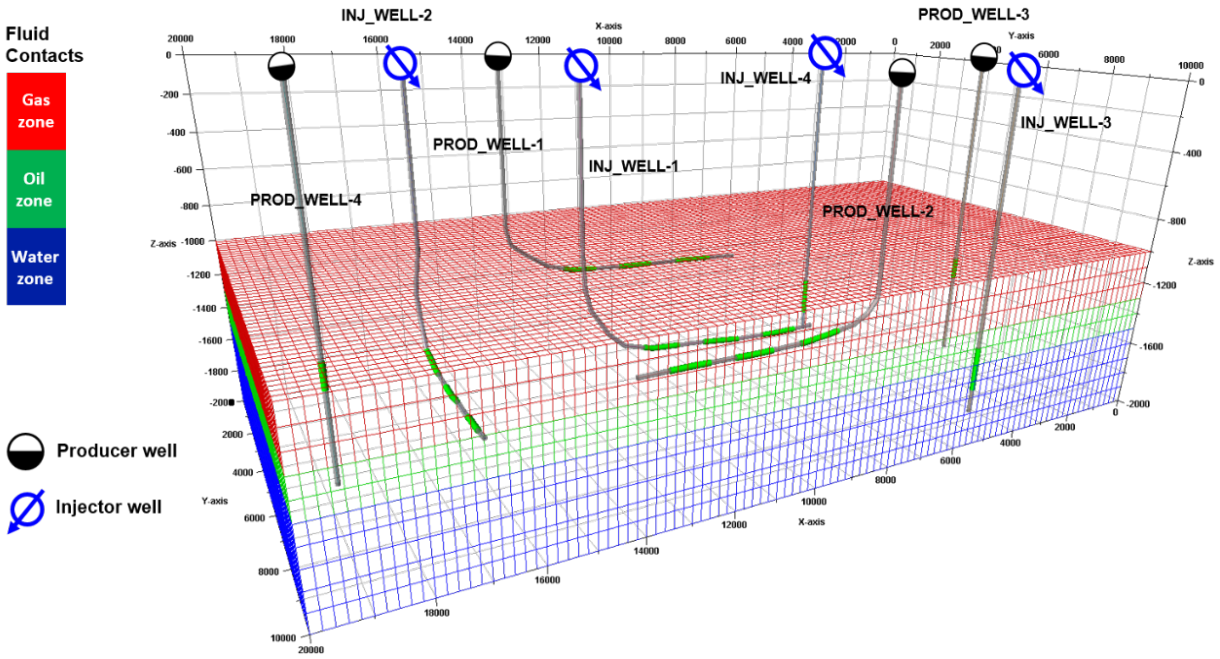
Fluid Contacts
Gas zone
Oil zone
Water zone
Producer well
Injector well
INJ_WELL-2
PROD_WELL-3
INJ_WELL-4
INJ_WELL-3
PROD_WELL-1
INJ_WELL-1
PROD_WELL-4
PROD_WELL-2
X-axis
Y-axis
Z-axis

FIGURE 13

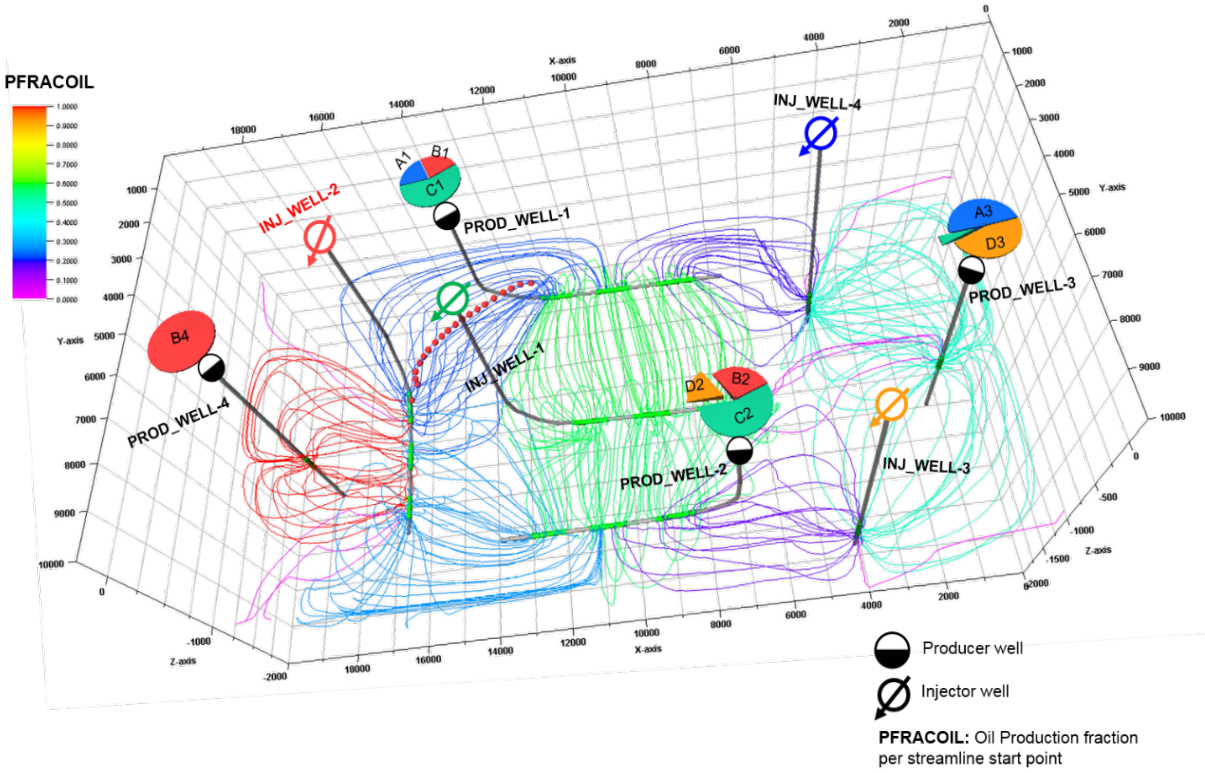
PFRACOIL
X-axis
Y-axis
Z-axis
INJ_WELL-2
INJ_WELL-4
INJ_WELL-1
INJ_WELL-3
PROD_WELL-1
PROD_WELL-2
PROD_WELL-3
PROD_WELL-4
A1
B1
C1
B4
D2
B2
C2
A3
D3
Producer well
Injector well
PFRACOIL: Oil Production fraction per streamline start point

FIGURE 14

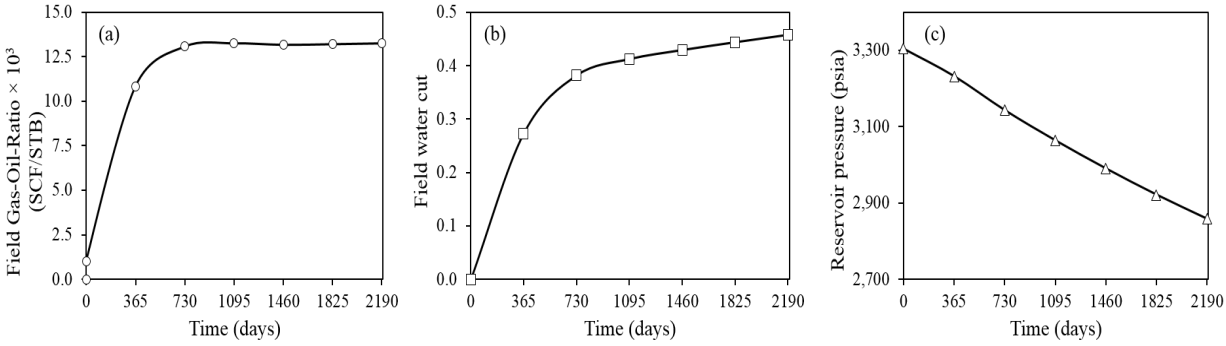
(a)
Field Gas-Oil-Ratio × 10³ (SCF/STB)
15.0
12.5
10.0
7.5
5.0
2.5
0.0
0
365
730
1095
1460
1825
2190
Time (days)
(b)
Field water cut
0.5
0.4
0.3
0.2
0.1
0.0
0
365
730
1095
1460
1825
2190
Time (days)
(c)
Reservoir pressure (psia)
3,300
3,100
2,900
2,700
0
365
730
1095
1460
1825
2190
Time (days)

FIGURE 15

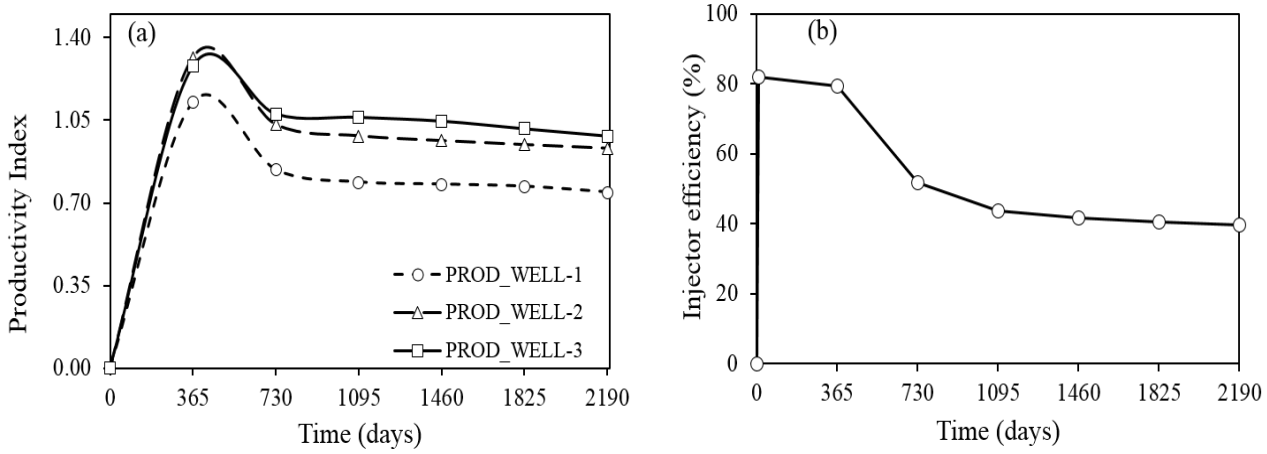
(a)
Productivity Index
1.40
1.05
0.70
0.35
0.00
0
365
730
1095
1460
1825
2190
Time (days)
PROD_WELL-1
PROD_WELL-2
PROD_WELL-3
(b)
Injector efficiency (%)
100
80
60
40
20
0
0
365
730
1095
1460
1825
2190
Time (days)

FIGURE 16

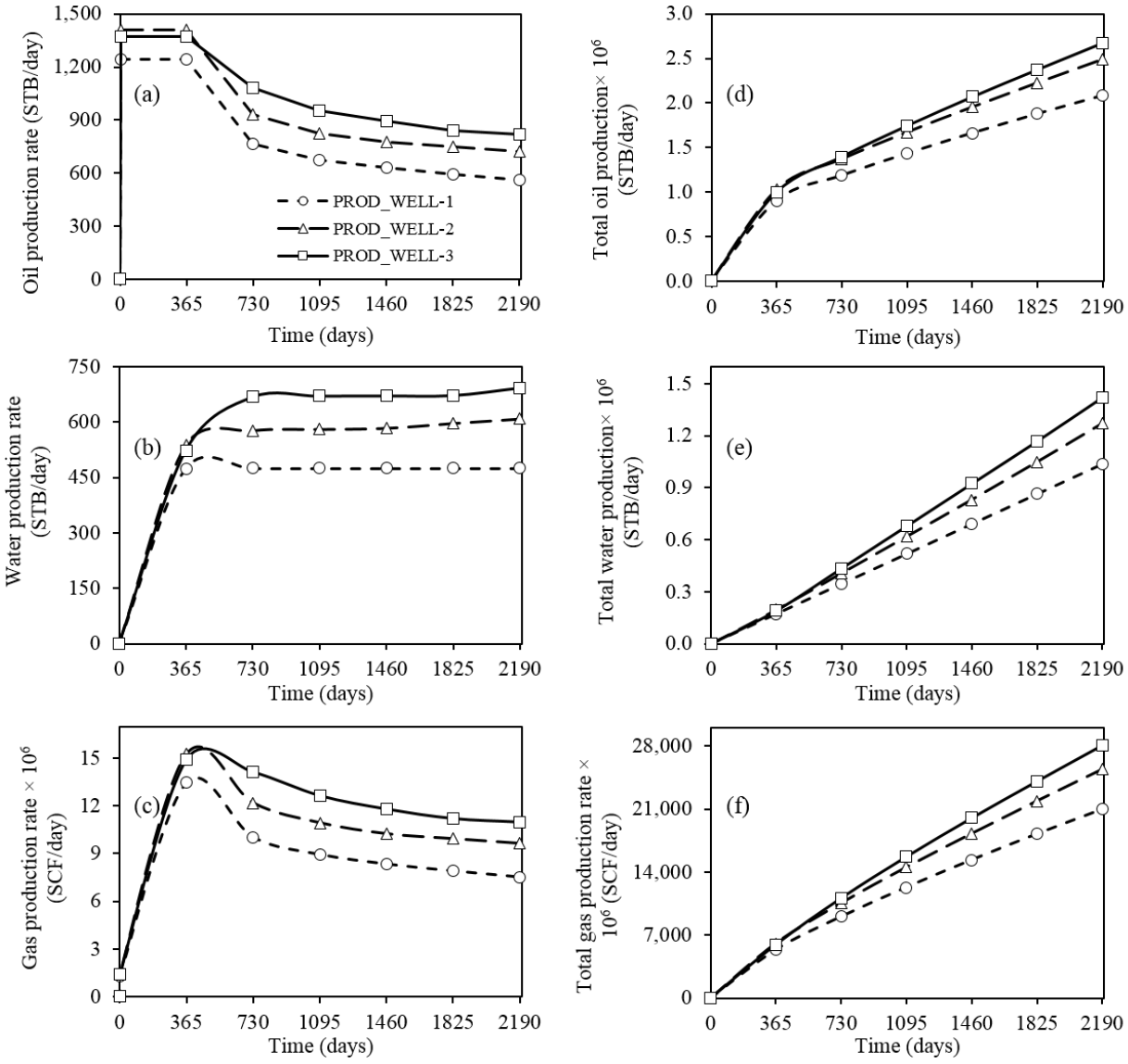
(a)
Oil production rate (STB/day)
1,500
1,200
900
600
300
0
PROD_WELL-1
PROD_WELL-2
PROD_WELL-3
0 365 730 1095 1460 1825 2190
Time (days)
(b)
Water production rate (STB/day)
750
600
450
300
150
0
0 365 730 1095 1460 1825 2190
Time (days)
(c)
Gas production rate × 10^6 (SCF/day)
15
12
9
6
3
0
0 365 730 1095 1460 1825 2190
Time (days)
(d)
Total oil production× 10^6 (STB/day)
3.0
2.5
2.0
1.5
1.0
0.5
0.0
0 365 730 1095 1460 1825 2190
Time (days)
(e)
Total water production× 10^6 (STB/day)
1.5
1.2
0.9
0.6
0.3
0.0
0 365 730 1095 1460 1825 2190
Time (days)
(f)
Total gas production rate × 10^6 (SCF/day)
28,000
21,000
14,000
7,000
0
0 365 730 1095 1460 1825 2190
Time (days)

FIGURE 17

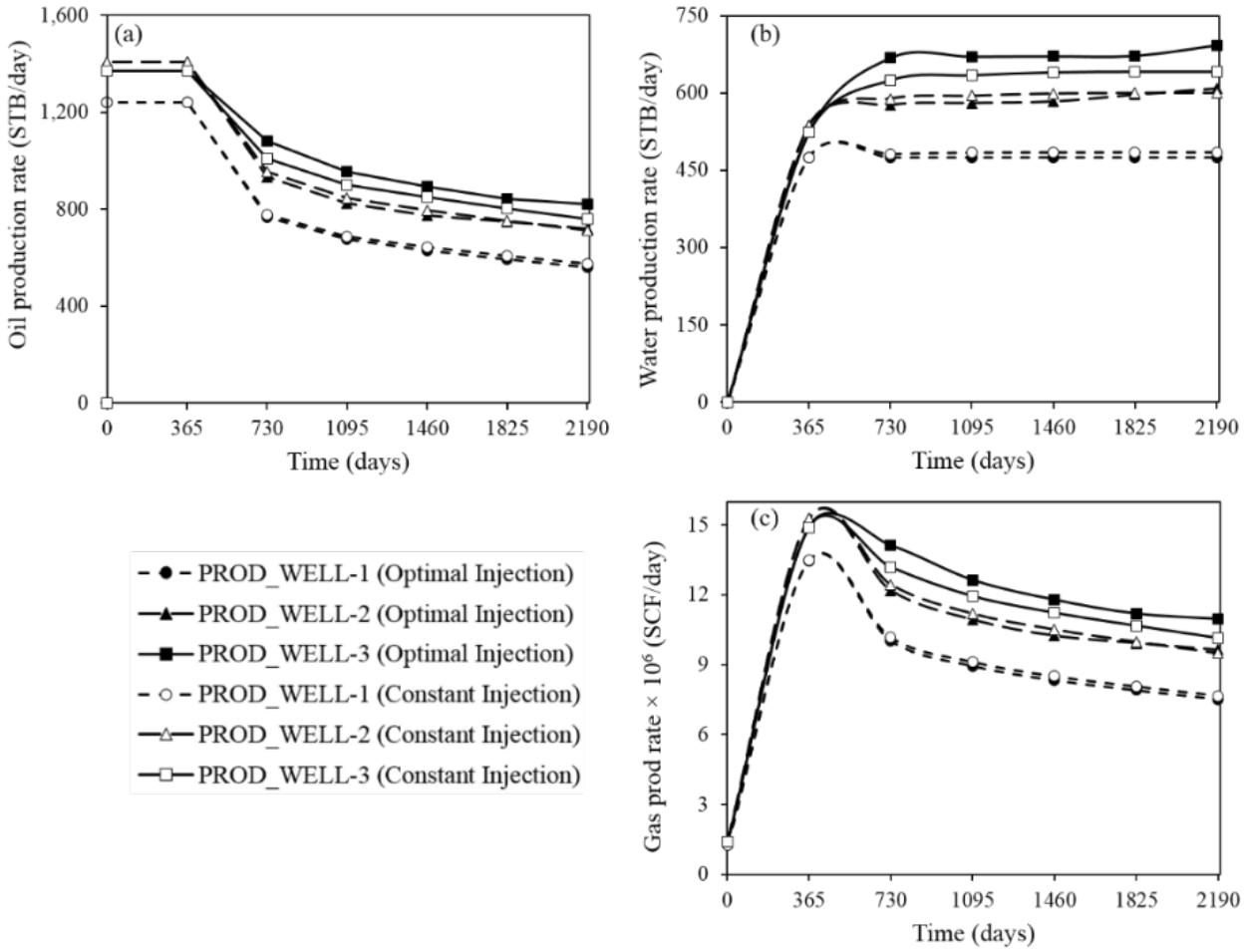
(a)
Oil production rate (STB/day)
1,600
1,200
800
400
0
0
365
730
1095
1460
1825
2190
Time (days)
(b)
Water production rate (STB/day)
750
600
450
300
150
0
Time (days)
(c)
Gas prod rate × 10^6 (SCF/day)
15
12
9
6
3
0
Time (days)
PROD_WELL-1 (Optimal Injection)
PROD_WELL-2 (Optimal Injection)
PROD_WELL-3 (Optimal Injection)
PROD_WELL-1 (Constant Injection)
PROD_WELL-2 (Constant Injection)
PROD_WELL-3 (Constant Injection)

FIGURE 18

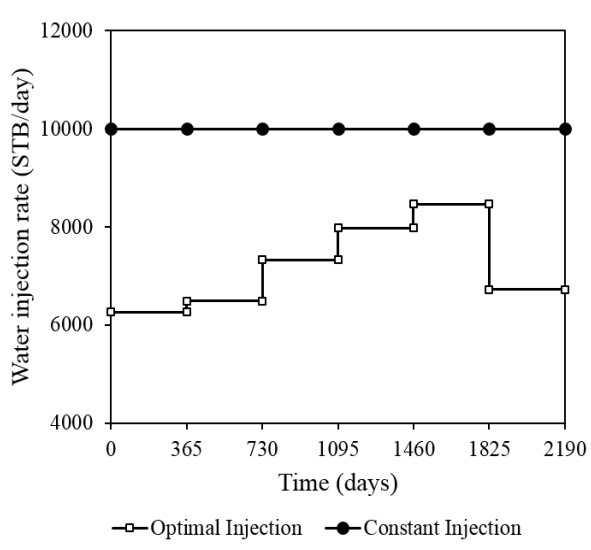
12000
10000
8000
6000
4000
Water injection rate (STB/day)
0
365
730
1095
1460
1825
2190
Time (days)
Optimal Injection
Constant Injection

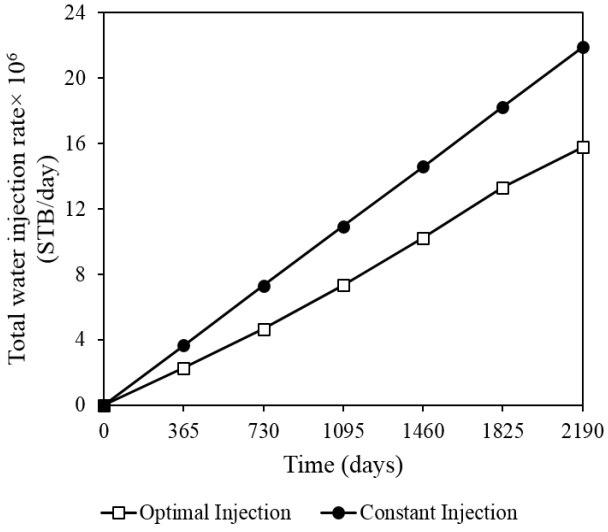
24
20
16
12
8
4
0
Total water injection rate× 10⁶ (STB/day)
0
365
730
1095
1460
1825
2190
Time (days)
Optimal Injection
Constant Injection

FIGURE 19

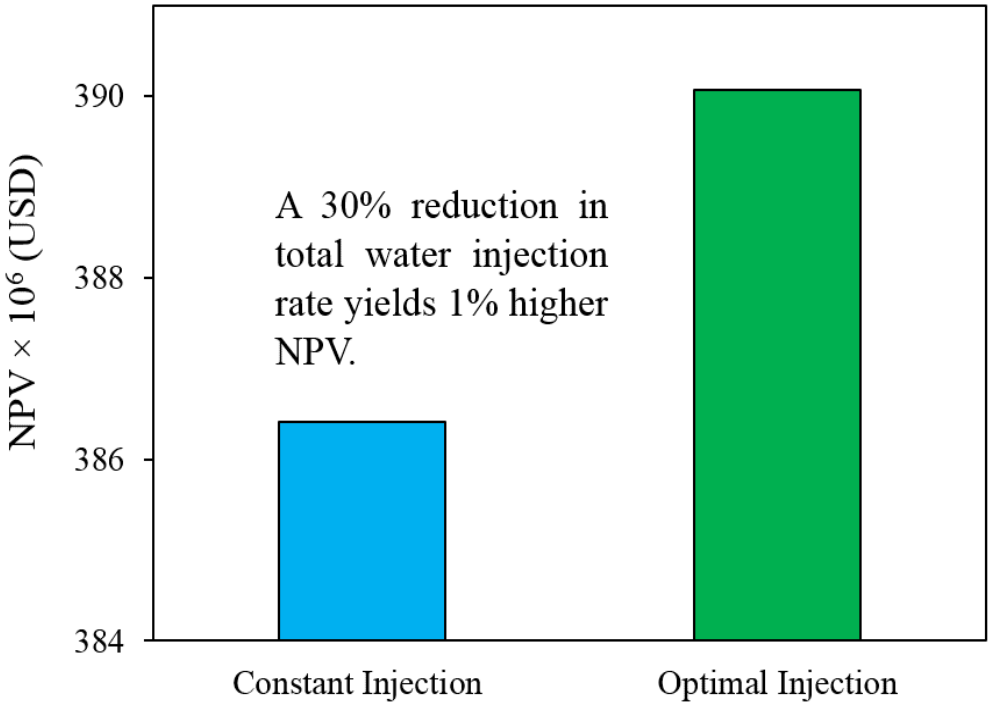
390
388
386
384
NPV × 10⁶ (USD)
A 30% reduction in total water injection rate yields 1% higher NPV.
Constant Injection
Optimal Injection

FIGURE 20

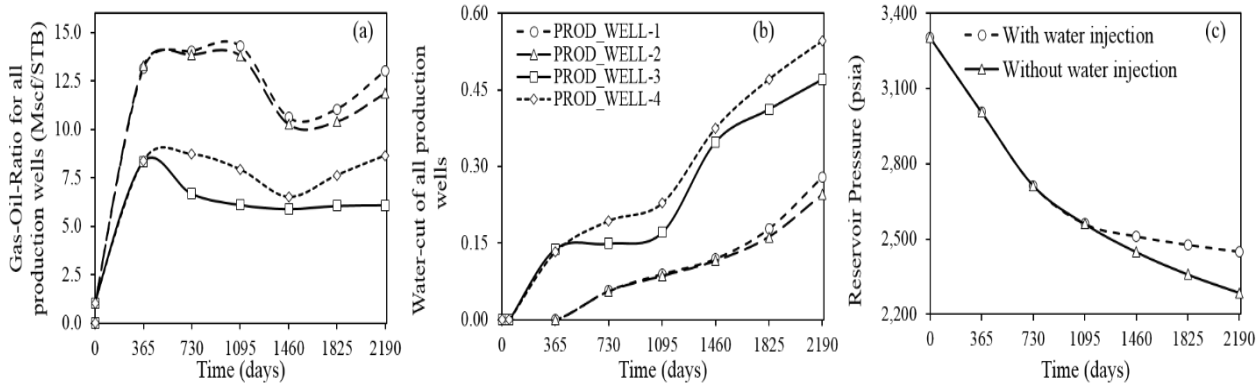
(a)
Gas-Oil-Ratio for all production wells (Mscf/STB)
15.0
12.5
10.0
7.5
5.0
2.5
0.0
0
365
730
1095
1460
1825
2190
Time (days)
(b)
PROD_WELL-1
PROD_WELL-2
PROD_WELL-3
PROD_WELL-4
Water-cut of all production wells
0.60
0.45
0.30
0.15
0.00
Time (days)
(c)
With water injection
Without water injection
Reservoir Pressure (psia)
3,400
3,100
2,800
2,500
2,200
Time (days)

FIGURE 21

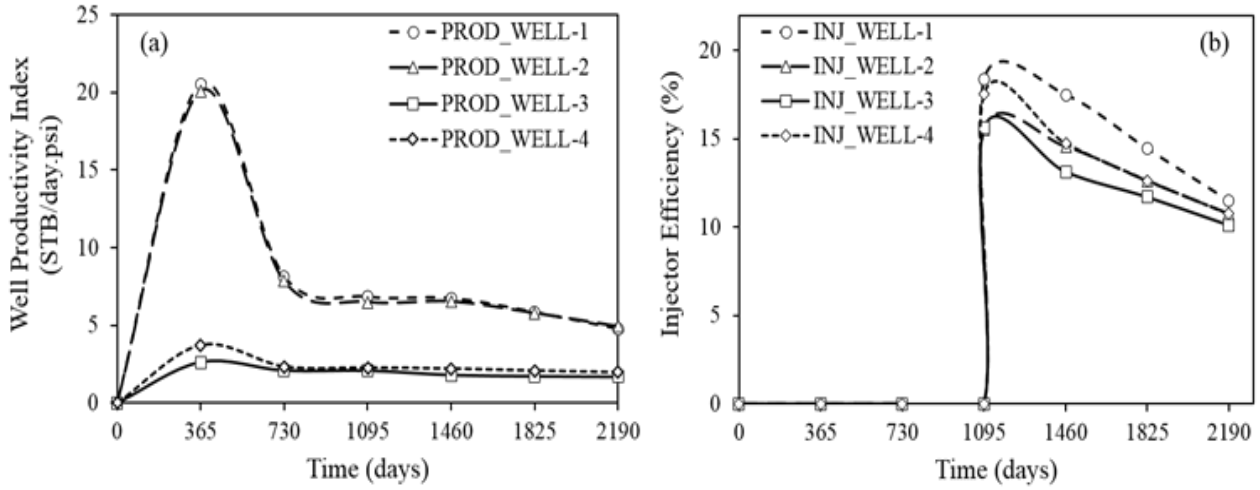
(a)
PROD_WELL-1
PROD_WELL-2
PROD_WELL-3
PROD_WELL-4
Well Productivity Index (STB/day.psi)
Time (days)
(b)
INJ_WELL-1
INJ_WELL-2
INJ_WELL-3
INJ_WELL-4
Injector Efficiency (%)
Time (days)

FIGURE 22

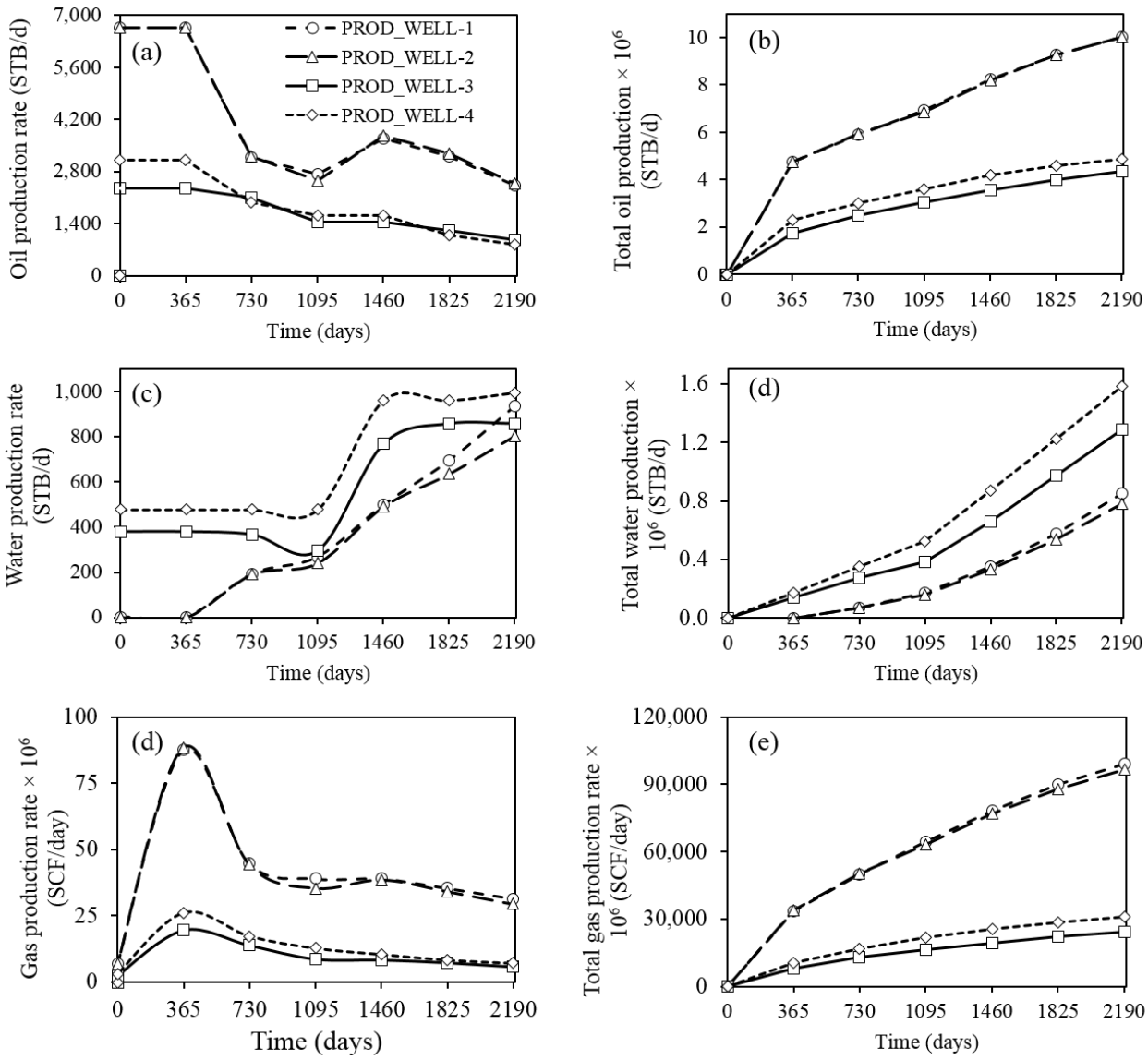
(a)
Oil production rate (STB/d)
7,000
5,600
4,200
2,800
1,400
0
PROD_WELL-1
PROD_WELL-2
PROD_WELL-3
PROD_WELL-4
0 365 730 1095 1460 1825 2190
Time (days)
(b)
Total oil production × 10⁶ (STB/d)
10
8
6
4
2
0
0 365 730 1095 1460 1825 2190
Time (days)
(c)
Water production rate (STB/d)
1,000
800
600
400
200
0
0 365 730 1095 1460 1825 2190
Time (days)
(d)
Total water production × 10⁶ (STB/d)
1.6
1.2
0.8
0.4
0.0
0 365 730 1095 1460 1825 2190
Time (days)
(d)
Gas production rate × 10⁶ (SCF/day)
100
75
50
25
0
0 365 730 1095 1460 1825 2190
Time (days)
(e)
Total gas production rate × 10⁶ (SCF/day)
120,000
90,000
60,000
30,000
0
0 365 730 1095 1460 1825 2190
Time (days)

FIGURE 23

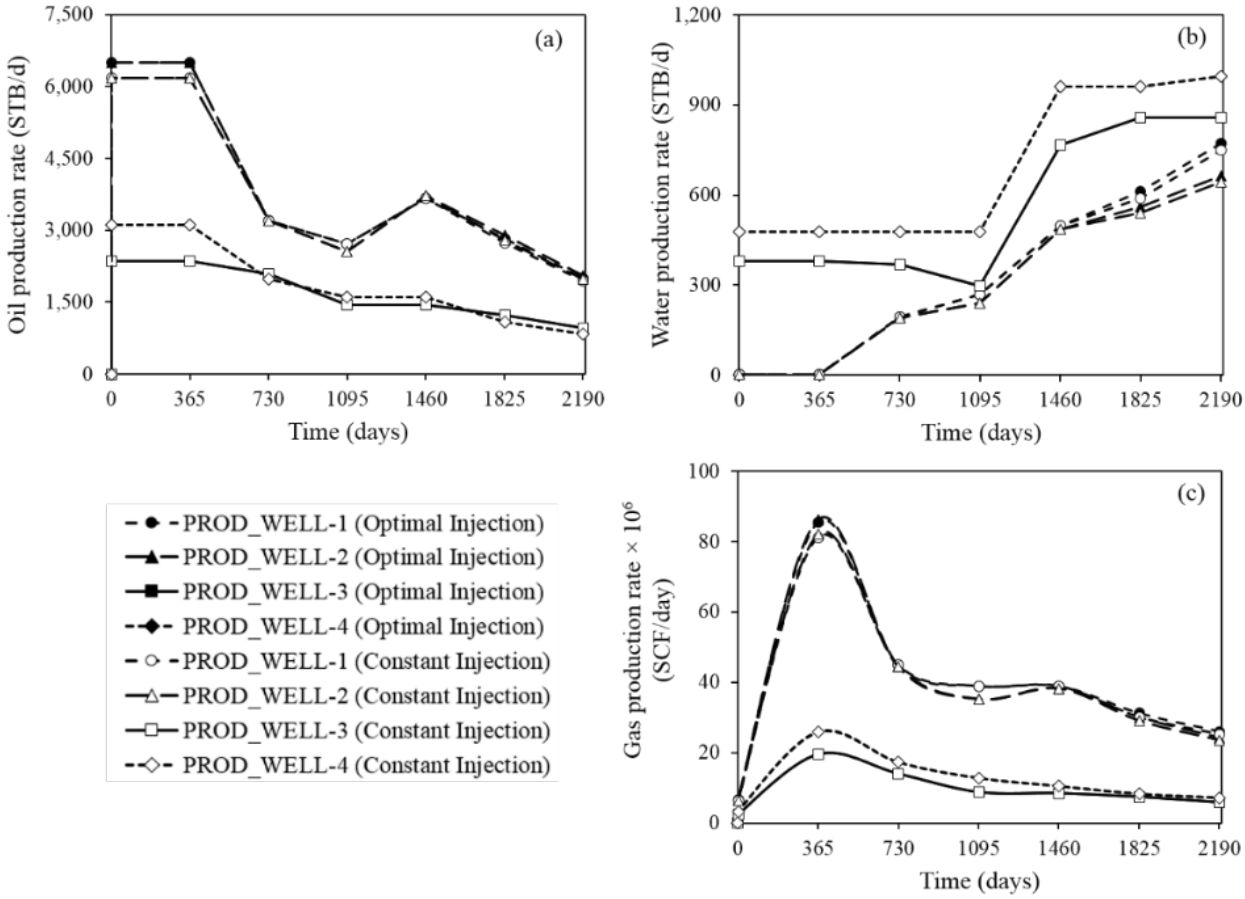
(a)
Oil production rate (STB/d)
7,500
6,000
4,500
3,000
1,500
0
0
365
730
1095
1460
1825
2190
Time (days)
(b)
Water production rate (STB/d)
1,200
900
600
300
0
Time (days)
(c)
Gas production rate × 10^6 (SCF/day)
100
80
60
40
20
0
Time (days)
PROD_WELL-1 (Optimal Injection)
PROD_WELL-2 (Optimal Injection)
PROD_WELL-3 (Optimal Injection)
PROD_WELL-4 (Optimal Injection)
PROD_WELL-1 (Constant Injection)
PROD_WELL-2 (Constant Injection)
PROD_WELL-3 (Constant Injection)
PROD_WELL-4 (Constant Injection)

FIGURE 24

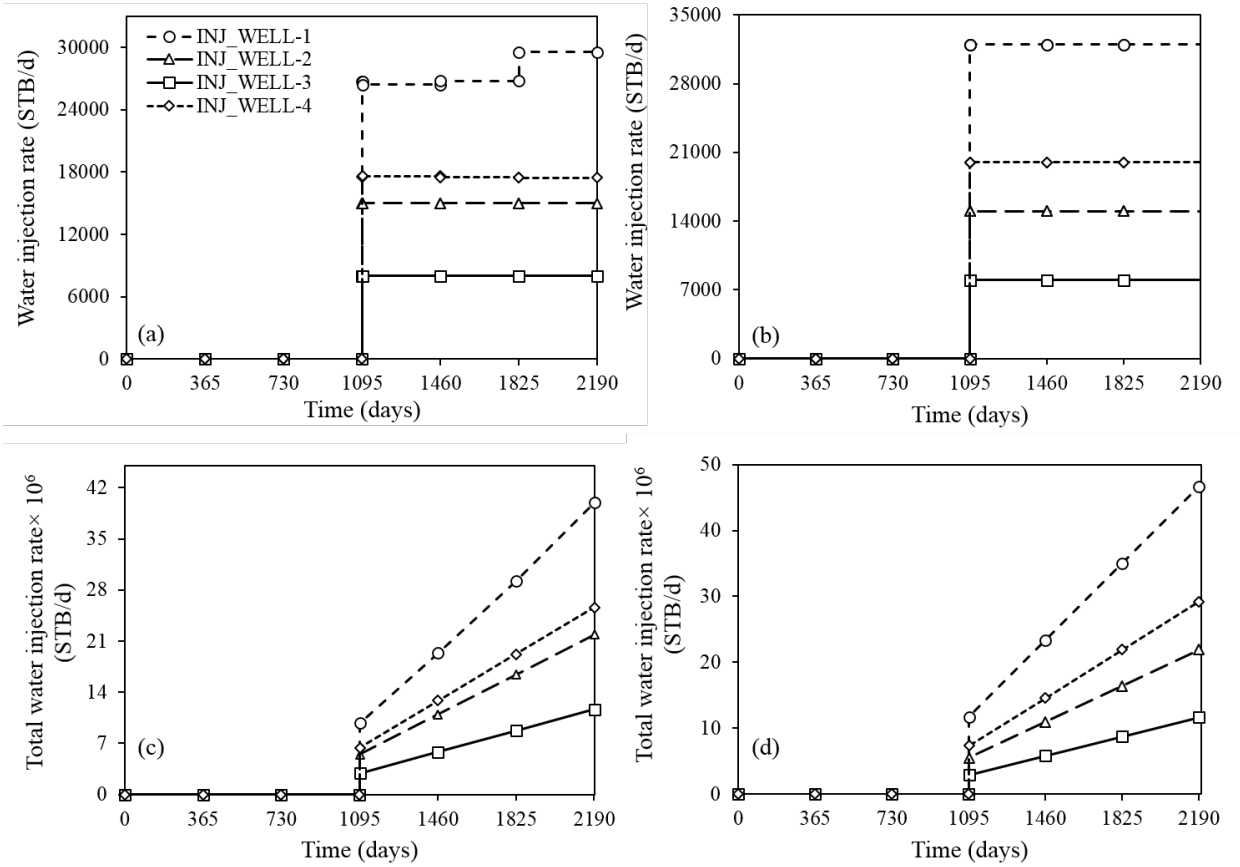
INJ_WELL-1
INJ_WELL-2
INJ_WELL-3
INJ_WELL-4
Water injection rate (STB/d)
Time (days)
(a)
(b)
Total water injection rate× 10^6 (STB/d)
(c)
(d)

FIGURE 25

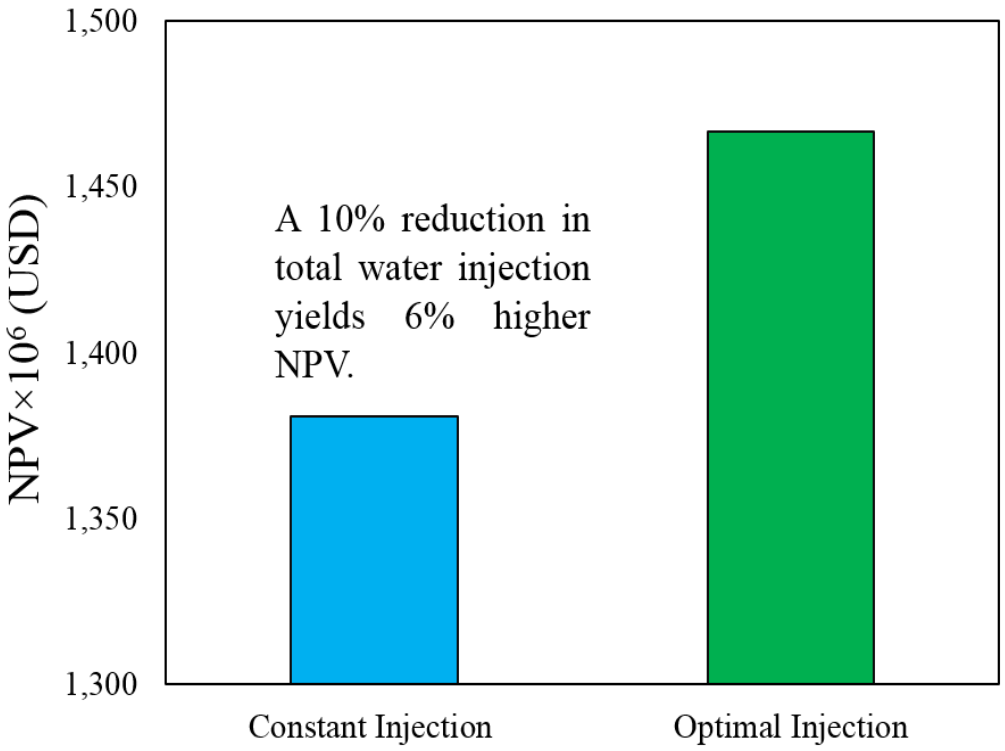
1,500
1,450
1,400
1,350
1,300
NPV×10⁶ (USD)
A 10% reduction in total water injection yields 6% higher NPV.
Constant Injection
Optimal Injection

FIGURE 26

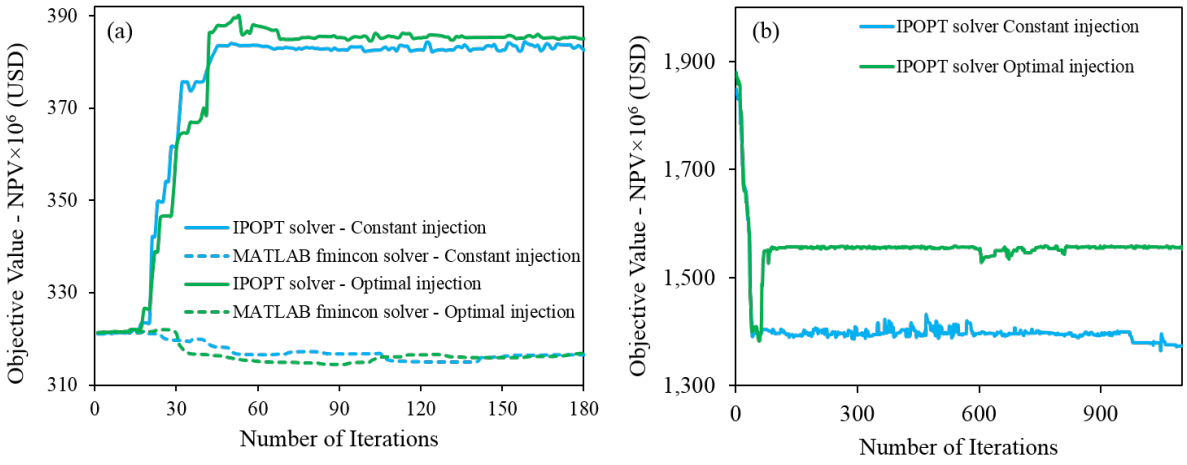
(a)
Objective Value - NPV×10⁶ (USD)
390
370
350
330
310
0
30
60
90
120
150
180
Number of Iterations
IPOPT solver - Constant injection
MATLAB fmincon solver - Constant injection
IPOPT solver - Optimal injection
MATLAB fmincon solver - Optimal injection
(b)
Objective Value - NPV×10⁶ (USD)
1,900
1,700
1,500
1,300
0
300
600
900
Number of Iterations
IPOPT solver Constant injection
IPOPT solver Optimal injection

LIST OF TABLE CAPTIONS

TABLE 1

Table 1: Fluid and reservoir properties

Fluid properties at reservoir conditions	*Value*
Gas density (kg/m^{-3})	0.8117
Oil density (kg/m^{-3})	801
Water density (kg/m^{-3})	1020.3
Gas viscosity (cP)	0.0214
Oil viscosity (cP)	0.4610
Water viscosity (cP)	0.3989
Gas formation volume factor (RB/STB)	0.854
Oil formation volume factor (RB/STB)	1.191
Water formation volume factor (RB/STB)	1.013
Gas compressibility (1/psi)	0.000251
Oil compressibility (1/psi)	0.000012
Water compressibility (1/psi)	0.00000273
Water salinity (ppm)	30000
Initial reservoir pressure (psia)	3300
Reservoir dimensions (100×50×10)	*Value*
DX (m)	20000
DY (m)	10000
DZ (m)	1000

TABLE 2

Table 2: Structure of data obtained for each well and pipeline from PIPESIM® at each timestep

P_{well} (psia)	$Q_{well,oil}$ (STB/day)	$Q_{well,gas}$ (MSCF/day)	$Q_{well,water}$ (STB/day)
t_1 = 365 days			
50	✓	✓	✓
….	✓	✓	✓
2500	✓	✓	✓
t_2 = 730 days			
50	✓	✓	✓
….	✓	✓	✓
2500	✓	✓	✓
:	:	:	:
t_n = 2190 days	✓	✓	✓

This table is generated for all producer wells and injector wells in the field. Note that the injector wells contain only a single fluid – water. Similar strategy is used for the pipelines in which the wellhead pressure column in the table is replaced with the pipeline pressure drop.

TABLE 3

Table 3: Injection and production well properties (CS 1)

Well	Type	Surface position, X (ft)	Surface position, Y (ft)	Perforation interval (ft)	
				Top	Bottom
INJ_WELL-1	Horizontal	9067	8774	1772 3769 6104	2779 4932 7111
PROD_WELL-1	Vertical	15000	8000	1331	1483
PROD_WELL-2	Vertical	14286	1891	1322	1471
PROD_WELL-3	Vertical	4475	4497	1329	1464

TABLE 4

Table 4: Computational summary (CS 1)

Property	Value
Number of producer wells	3
Number of injector wells	1
Number of pipelines	1 major pipeline
Number of objective functions	1
Number of time step discretisation (6-year horizon)	6
Number of constraints (nonlinear, linear, equality, inequality)	159
Total number of variables	114

TABLE 5

Table 5: Injection and production well properties (CS 2)

Well	Type	Surface position, X (ft)	Surface position, Y (ft)	Perforation interval (ft)	
				Top	Bottom
INJ_WELL-1	Horizontal	12957	4788	2813 4494 6287	3766 5520 7303
INJ_WELL-2	Horizontal	16090	2681	1884 3354 4940	2774 4168 5591
INJ_WELL-3	Vertical	4135	8697	1576	1849
INJ_WELL-4	Vertical	4168	1678	1620	1870
PROD_WELL-1	Horizontal	13543	1300	2620 4257 6017	3529 5219 7118
PROD_WELL-2	Horizontal	7098	8138	2328 4106 5679	3345 5046 6634
PROD_WELL-3	Vertical	1301	4942	1328	1465
PROD_WELL-4	Vertical	18737	5324	1323	1472

TABLE 6

Table 6: Computational summary (CS 2)	
Property	**Value**
Number of producer wells	4
Number of injector wells	4
Number of pipelines	2 major pipelines
Number of objective functions	1
Number of time step discretisation (6-year horizon)	6
Number of constraints (nonlinear, linear, equality, inequality)	252
Total number of variables	198

TABLE 7

Table 7: Solver performance analysis

	Case Study 1		Case Study 2	
Solver	**Average solution time (sec)**	**Average number of Iterations**	**Average solution time (sec)**	**Average number of Iterations**
IPOPT	21	600	133	2600
MATLAB fmincon	>50	>1000	772	> 4000

Reported data is for a single set of initial guesses for both the optimised and constant injection rates.